Optogenetic modulation of the corticostriatal circuitry in chronic pain

Inês Costa Laranjeira

Departamento de Biomedicina

Faculdade de Medicina da Universidade do Porto

PORTO, 2017

Dissertação apresentada à Faculdade de Medicina da Universidade do Porto para a obtenção do grau de Mestre em Neurobiologia

Orientação de Helder Rui Cardoso da Cruz

Co-orientação de Clara Maria Pires Costa de Bastos Monteiro

Agradecimentos

Pela contribuição que tiveram, de forma direta ou indireta, na realização deste projeto de tese, pretendo aqui expressar os meus agradecimentos a várias pessoas.

Agradeço ao Professor Doutor Vasco Galhardo por me ter dado a oportunidade de me juntar ao laboratório por si liderado para levar a cabo o projeto da minha tese de mestrado, do qual resultou esta dissertação. Agradeço ao meu orientador, Doutor Helder Cruz, pelo acompanhamento e orientação constantes ao longo de todo o projeto e à minha co-orientadora, Professora Doutora Clara Monteiro, pela importante contribuição que teve em diferentes fases do projeto.

Agradeço à Doutora Mafalda Sousa pela amizade, que trouxe consigo muitos conselhos sábios. Agradeço ao Professor Doutor Carlos Reguenga por ser para mim um verdadeiro mentor do espírito científico. Agradeço ainda à Professora Doutora Deolinda Lima pelo empenho e profissionalismo na direção deste projeto que é o Mestrado em Neurobiologia.

Agradeço a todos os meus colegas de mestrado e a todos os meus amigos de sempre por me manterem sã e feliz, independentemente das dificuldades.

Agradeço aos meus pais e restante família pelo amor e apoio incondicionais.

Table of contents

Abbreviations

AAV	Adeno associated virus
ACC	Anterior cingulate cortex
ANOVA	Analysis of variance
AP	Anterio-posterior
ChR	Channelrhodopsin
COH2	Quadratic coherence
DNMS	Delayed non-matching to sample
DV	Dorso-ventral
eNpHR	Enhanced *Natronomonas pharaonic* halorhodopsin
eNpHR3.0	Third generation *Natronomonas pharaonic* halorhodopsin
fMRI	Functional magnetic resonance imaging
HR	Halorhodopsin
hSyn	Human synapsin-1
ITI	Inter-trial interval
KS	Kolmogorov-Smirnov
KS2	2-sample Kolmogorov-Smirnov
KW	Kruskal-Wallis
LFP	Local field potential
ML	Medio-lateral
mPFC	Medial prefrontal cortex
NAc	*Nucleus accumbens*
NAcc	*Nucleus accumbens* core
NMDA	N-methyl-D-aspartate
NpHR	*Natronomonas pharaonic* halorhodopsin
PBS	Phosphate buffered saline
PDC	Partial directed coherence
PETH	Perievent-time histogram
PFC	Prefrontal cortex
PL	Prelimbic
PSD	Power spectral density
S1	Primary somatosensory cortex

S2	Secondary somatosensory cortex
SEM	Standard error of the mean
SNI	Spared nerve injury
sWM	Spatial working memory
TTL	Transistor-transistor logic
VTA	Ventral tegmental area
WM	Working memory

Abstract

Chronic pain is accompanied by maladaptive changes at the cellular, structural and functional level, affecting multiple brain regions. These changes are thought to underlie the disruption of several cognitive functions, which are commonly reported by patients and observed in chronic pain animal models. Interactions between the medial prefrontal cortex (mPFC) and the *nucleus accumbens* (NAc) are particularly important in the promotion of goal-directed behaviors, which subserves many aspects of behavior performance. During chronic pain, both the mPFC and NAc brain regions were shown to have altered activity, and corticostriatal functional connectivity seems to be enhanced in humans, prior to pain chronification. Despite all knowledge, the corticostriatal reorganization in chronic pain conditions is not completely understood. In addition, the impact of this reorganization in cognitive functions that rely on the correct functioning of these areas has been poorly explored.

The present work aimed to investigate the role of the corticostriatal circuitry in the nociceptive information processing, and chronic pain-related spatial working memory (sWM) deficits. To address this issue, the activity of the glutamatergic pyramidal neurons projecting from the prelimbic (PL) mPFC to the NAc *core* (NAcc) was optogenetically modulated in a rodent model of neuropathic pain - spared nerve injury (SNI). The impact of the delay period inhibition of the corticostriatal circuit on sWM was assessed in the behavioral performance of both pre-trained and non-trained challenges of a delayed non-matching to sample (DNMS) sWM task. The impact of the optogenetic inhibition of the corticostriatal circuit was further evaluated on the mechanical sensitivity level, using the von Frey filaments test. In addition to the performed behavioral analyses, extracellular spiking activity and local field potentials were recorded simultaneously from the PL-mPFC and NAcc regions.

The present results revealed enhanced levels of corticostriatal connectivity after the induction of the SNI neuropathic pain model. It was also found that selective corticostriatal circuit optogenetic inhibition during the delay period resulted in enhanced performance levels of the SNI-treated animals during non-trained DNMS challenges, but this effect was not associated with alterations in pain perception. However, the homolog optogenetic modulation of the circuit did not have an impact on the performance levels during pre-trained DNMS challenges.

Together, these findings suggest that restoring the balance of corticostriatal circuitry local activity may be an important therapeutic strategy to reverse WM deficits observed during painful syndromes.

Keywords: chronic pain; working memory; corticostriatal circuitry; optogenetics.

Sumário

A dor crónica é acompanhada por alterações mal-adaptativas ao nível celular, estrutural e funcional, afetando múltiplas áreas do cérebro. Pensa-se que estas alterações estejam na base dos défices cognitivos comummente relatados por pacientes e observados em modelos animais de dor crónica. As interações entre o córtex pré-frontal medial (mPFC) e o núcleo *accumbens* (NAc) são particularmente importantes na promoção de comportamentos direcionados ao um objetivo, contribuindo para variados aspetos da performance comportamental. Foi mostrado que durante a dor crónica, o mPFC e o NAc têm a sua atividade alterada e, recentemente, foi visto que a conetividade funcional corticoestriatal está aumentada em humanos, antes da cronificação da dor. Apesar do conhecimento reunido, a reorganização corticoestriatal em estados de dor crónica não é completamente entendida. Para além disso, o impacto que esta reorganização tem nas funções cognitivas dependentes do correto funcionamento destas áreas tem sido pouco explorado.

O presente trabalho pretendeu investigar o papel do circuito corticoestriatal no processamento da informação nociceptiva e nos défices de *working memory* de referência espacial (sWM) associados à dor crónica. Para isso, a atividade dos neurónios piramidais glutamatérgicos que da região do pré-límbico (PL) do mPFC projetam para a zona do *core* do NAc (NAcc) foi modulada optogeneticamente num modelo de dor neuropática – *spared nerve injury* (SNI). O impacto da inibição do circuito corticoestriatal durante o período de *delay* na sWM foi avaliado através da performance comportamental em desafios pré-treinados e não treinados de uma tarefa *delayed non-matching to sample* (DNMS) de sWM. O impacto da inibição optogenética do circuito corticoestriatal nos níveis de sensibilidade mecânica foi também avaliado, com o teste dos filamentos de von Frey. Para além da análise comportamental, também foram feitos registos de potenciais de ação e potenciais de campo locais, simultaneamente no PL-mPFC e NAcc.

Os presentes resultados mostraram que os níveis de conetividade corticoestriatal estão aumentados depois da indução do modelo SNI de dor neuropática. Também se verificou que a inibição optogenética seletiva do circuito corticoestriatal durante o período de *delay* resultou num aumento dos níveis de performance de animais SNI em desafios DNMS não treinados, mas este efeito não foi associado a alterações na perceção da dor. No entanto, homóloga modulação optogenética do circuito não teve um impacto nos níveis de performance em desafios DNMS pré-treinados.

Estes resultados sugerem que o restabelecimento da atividade local do circuito corticoestriatal pode ser uma importante estratégia terapêutica na reversão de défices de WM observados em síndromes dolorosas.

Conceitos-chave: dor crónica; *working memory*; circuito corticoestriatal; optogenética.

I. Introduction

1.1. Working memory

Working memory (WM) was defined as the storage and manipulation of information in mind over a short period of time, when it is no longer present (Baddeley, 2012). This faculty is constantly demanded to successfully guide behavior and was considered "a major achievement of evolution" (Goldman-Rakic, 1987). Early studies in monkeys led to the conclusion that the PFC has an important role in mediating WM. Lesion to or temporary inactivation of the PFC resulted in impaired performance of tasks involving WM in monkeys (Jacobsen, 1935, Bauer and Fuster, 1976, Funahashi et al., 1993). These deficits were also reproduced in rats (Granon et al., 1994, Kolb et al., 1994, Seamans et al., 1995, Porter and Mair, 1997). Importantly, studies on humans based on lesions of the PFC or functional magnetic resonance imaging (fMRI) analysis also implicate the PFC in WM (Muller et al., 2002, Voytek and Knight, 2010).

Electrophysiological recordings of PFC neurons in monkeys revealed persistent activity during the delay period of a delayed-response task (Fuster and Alexander, 1971, Funahashi et al., 1989, Miller et al., 1996). It was proposed that this activity codes task-relevant information and that it is fundamental for the maintenance of stimulus representations in WM (Courtney et al., 1997, Riley and Constantinidis, 2015). However, besides the PFC, other brain areas have persistent activity during the delay period, including the parietal cortex, sensory cortices and subcortical structures, including the caudate, hippocampus and thalamus (Gazzaley et al., 2004, Christophel et al., 2017). Furthermore, stimulus-specific activity was also found in other cortical regions, such as the primary visual cortex and other sensory regions, depending on the modality of the stimulus (Harrison and Tong, 2009). There is still no consensus about the function of the PFC persistent activity and even about its necessity for information retention in WM (D'Esposito and Postle, 2015). A well supported hypothesis proposes that PFC persistent activity serves the function of top-down controller over other brain areas, recruited during the delay period, thus having an indirect role on storage being held in other structures (Gazzaley and Nobre, 2012, D'Esposito and Postle, 2015, Christophel et al., 2017). That is, the PFC is thought to exert a central modulatory role, enhancing task-relevant information and suppressing task-irrelevant information, which is not a property of sensory cortices (Gazzaley and Nobre, 2012). Furthermore, the PFC coordinates the executive aspect of WM. It is in

strong communication with non-sensory areas in the basal ganglia, limbic system and brainstem, particularly important both conveying information regarding internal goals, reward values, and abstract rules and in mediating goal-directed behavior during WM (Miller and Cohen, 2001).

Rhythmic patterns of activity in the brain are thought to contribute to the coordination of distinct brain areas during WM. It is hypothesized that synchronization between neuronal oscillations potentiates efficient transmission of information between distributed neuronal populations (Fries, 2005). In humans, several studies point to a correlation between the enhanced amplitude of oscillatory activity in the θ (4-9 Hz), α (9-12 Hz), and γ (30-100 Hz) bands and maintenance of WM information (reviewed in Roux and Uhlhaas, 2014). For instance, synchronization of neuronal oscillations in the frontoparietal areas was shown to be stable and sustained during the retention period of a visual WM task and was content-specific (Palva et al., 2010, Salazar et al., 2012), corroborating the role of synchronous oscillatory activity in WM.

In rodents, hippocampal θ activity is a prominent type of oscillation during voluntary locomotor behavior which has been particularly well studied (Buzsaki, 2002). Firing of individual neurons in the medial PFC (mPFC) was shown to occur phase locked to hippocampal θ rhythm during diverse behavioral tasks (Hyman et al., 2005, Siapas et al., 2005). Theta-frequency entrainment of mPFC firing was shown to be modulated by behavioral demands and correlated with performance levels during a spatial WM (sWM) task (Jones and Wilson, 2005, Hyman et al., 2010, O'Neill et al., 2013). Besides the mPFC, other areas are entrained to hippocampal-θ rhythm, as is the case of the amygdala and striatum (Pare and Gaudreau, 1996, Berke et al., 2004). Overall, coherent θ activity is thought to be important in the communication between distinct brain regions (Buzsaki, 2002), which seems to be crucial during WM.

In conclusion, WM is a cognitive process that is not restricted to one anatomical place and instead is distributed through the brain, involving distinct regions. The PFC is thought to play a central role in coordinating this orchestra but, simultaneously, it also seems to depend on the intercommunication with other areas, where preprocessing of information occurs. The understanding of WM mechanisms is not complete and, in particular, the mechanisms by which WM is impaired in pathological states such as chronic pain are not fully understood and deserve further investigation (Moriarty et al., 2011).

1.1.2. Spatial working memory tasks in rodents

Rodents are widely used to study WM. Motivated by instinctive or learned rewarding behaviors, rats and mice can be tested for their capacity to actively maintain information during a short period of time, to further guide behavior.

A classical sWM task is the *Morris water maze* task. The animal should repeat the pathway followed in a first trial, to find a hidden platform in the water maze, and relieve its own stress. While in the first trial, the animal finds the platform by extensively exploring the maze, in the second trial, the animal relies on sWM to find it faster (Morris et al., 1986).

The *radial arm maze* task is based on the natural tendency of rodents to search for food in yet unvisited places, a behavior which results in a better outcome for the animal. When positioned on a central platform with access to several identical baited arms, the animal tends to visit the unvisited arms first, where it can still find the bait, avoiding visited arms. sWM allows the animal to discriminate between visited and unvisited arms in a session (S. Olton and J. Samuelson, 1976).

In delayed alternation tasks, the animal is rewarded for alternating a certain behavior. The *T-maze* task takes advantage of the tendency of rodents to spontaneously alternate arm visits in repeated exposures to the maze. When a delay period is interposed between the first and second runs in the T-maze, the rat relies on sWM to decide for the alternative arm, the rewarding behavior (Sanchez-Santed et al., 1997). Other tasks resemble the T-maze task concept, by rewarding the rat for following the alternative pathway, in mazes of varying shapes (Baeg et al., 2003, Cardoso-Cruz et al., 2013, Cardoso-Cruz et al., 2014).

Another important type of delayed alternation tasks is referred to as *delayed non-matching to sample* (DNMS). In the DNMS task, the alternated behavior is the approach to a given sample. The animal is presented with a spatial sample, which becomes absent during a delay period. In the end of the delay period, the animal is presented with two (or more) options, containing the initial sample, and it is rewarded for choosing the alternative sample. This task requires WM for its solution (Olton et al., 1979, Gal et al., 1997, Dunnett et al., 1999). The task usually takes place in an operant chamber, in which the spatial samples are usually levers or nose-pokes. Being an operant task and possibly fully automatized, the experimenter interference in both learning and testing is reduced. This is also an advantage in experiments involving optogenetic stimulation. Finally, this task allows the establishment of a fixed delay period, which might be convenient in some analysis.

1.2. Chronic pain - related cognitive impairments

According to the International Association for the Study of Pain, pain is "an unpleasant sensory and emotional experience associated with actual or potential tissue damage" (https://www.iasp-pain.org/Taxonomy). Pain experience has a protective role towards damaging stimuli. For instance, it triggers reflexive behaviors to escape, terminate and avoid tissue damage and potentiates learning. However, pain might persist longer than biologically advantageous, becoming pathological and potentially chronic, as is the case of neuropathic pain (Costigan et al., 2009). Neuropathic pain results from a "lesion or disease of the somatosensory system" (Jensen et al., 2011). Such circumstances might be associated with diseases including diabetes, multiple sclerosis, and Parkinson's disease may arise after contact with neurotoxic chemicals, infection, or, very commonly, after traumatic damage to the peripheral or central nervous system. Patients report hyperalgesia, allodynia and spontaneous pain, this having a great impact on life quality (Costigan et al., 2009). However, the transition to neuropathic pain is not inevitable; it is thought that several factors might potentiate an imbalance between adaptive and maladaptive reactions occurring after injury (Costigan et al., 2009). Overall, and transversally to other forms of chronic pain, there is an increased excitability and loss of inhibition both in the periphery, spinal cord, and brain (Costigan et al., 2009).

In non-pathological conditions, nociceptive information coming from the periphery is transmitted by primary afferent neurons to the dorsal horn of the spinal cord. Ascending pathways target different areas in the brainstem and forebrain, where nociceptive stimuli are integrated and modulated. Neuroimaging studies consistently show that pain experience is correlated with increased activity in the primary and secondary somatosensory cortices (S1 and S2), insular cortex, anterior cingulate cortex (ACC), and other areas of the PFC, and subcortically in the thalamic nuclei, basal ganglia and cerebellum (Apkarian et al., 2005, Neugebauer et al., 2009). These brain structures (among others identified) constitute the so-called "pain-matrix" and are thought to have a role in the conscious and aware perception of pain, encoding sensory-discriminative and affective-cognitive aspects of pain (Tracey and Mantyh, Melzack and Wall, 1965, Price, 2000, Bushnell et al., 2013).

Neuropathic pain is accompanied by changes occurring at the cellular, structural and functional level, in the nociceptive system (Kuner and Flor, 2017). Inflammation, peripheral sensitization, and central sensitization processes occur (Costigan et al., 2009, von Hehn et al., 2012). Increased nociceptive inputs from the periphery to the dorsal horn of the spinal cord induce synaptic strengthening via long-term potentiation mechanisms (Woolf, 2011). Synaptic

plasticity has also been reported in supraspinal areas including the ACC, insular cortex, thalamus, amygdala, the S1 and the mPFC (Luo et al., 2014, Kuner and Flor, 2017). A direct consequence of central sensitization is that pain perception is no longer directly dependent on the peripheral noxious stimulus. On the contrary, pain perception is exacerbated and no longer serves a protective purpose (Woolf, 2011). Maladaptive functional plasticity occurring in the nociceptive network also includes morphological and structural changes, alterations in connectivity and changes in activity patterns (Kuner and Flor, 2017). Due to the redundancy of cerebral circuits, plastic changes occurring across the nociceptive system in neuropathic pain are believed to impact other brain functions, as is the case of the cognitive function (Hart et al., 2000).

Patients suffering from chronic pain commonly complain of cognitive impairments, which add significant difficulties to their daily life. Reported cognitive deficits were shown to be directly related to pain severity (Weiner et al., 2006). It is hypothesized that cognitive impairments associated with chronic pain are a consequence of limited resources in the brain, which are continuously solicited by pain processing and, thus, limit cognitive processing (Eccleston and Crombez, 1999). Many clinical and preclinical studies refer impairments in attention, learning, memory, executive function, information processing and psychomotor speed, associated with chronic pain conditions (reviewed in Moriarty et al., 2011).

WM normal functioning is fundamental to successfully pursue with many tasks of daily activity. Clinical studies report that chronic pain conditions lead to disruptions in WM capacity, as assessed by several tests and self-report (Jamison et al., 1988, Lewis et al., 2004, Dick and Rashiq, 2007, Lee et al., 2010, Oosterman et al., 2010, Oosterman et al., 2011). Several studies in animals also showed that the induction of both inflammatory (Cain et al., 1997, Lindner et al., 1999) and neuropathic (Leite-Almeida et al., 2009, Hu et al., 2010, Ren et al., 2011, Cardoso-Cruz et al., 2013, Cardoso-Cruz et al., 2014) chronic pain resulted in impaired performance in different WM tasks.

1.2.1. Peripheral neuropathic pain animal models

The study of neuropathic pain in human subjects is highly limited, because of the high variability of neuropathies and the difficulty to recruit large numbers of patients. Different animal models were developed in rodents that result in reproducible neuropathic pain symptoms and mimic neuropathies of different etiologies. Early development of peripheral nerve injury models resulted from the need to reproduce chronic pain symptoms in animals

and elucidate underlying mechanisms, which could not be studied with the existent acute pain models.

Wall and Gutnick performed a complete transection of the rat sciatic nerve to induce neuroma formation (Wall and Gutnick, 1974). As a consequence of complete denervation, intense autotomy behavior was described, which is thought to reflect spontaneous pain and mimic *anesthesia dolorosa* (pain in the absence of sensory input) observed in patients. However, besides this spontaneous behavior, hyperalgesia and allodynia symptoms are not easy to measure in this model, as there is no sensitivity to an applied stimulus (Wall et al., 1979). Moreover, complete transection of a nerve is rare and partial lesions are more common in clinical neuropathy. After this model, several were developed in which partial nerve lesion is induced.

In the chronic constriction injury model, four tight ligations are placed around the common sciatic nerve (Bennett and Xie, 1988). A variant of this model consists of the ligation of the common peroneal branch of the sciatic nerve (Vadakkan et al., 2005). Partial lesion of the sciatic nerve was also achieved through ligation of 1/3 to 1/2 of the nerve thickness (Seltzer et al., 1990). Common to models involving ligation of the nerve, there is some variation in the degree of the induced lesion, which is mainly explained by the variable tightness of the ligation and type of used suture material (Jaggi et al., 2011). The spinal nerve ligation model consists of the tight ligation of L5 or L5 and L6 spinal nerves of the rat, and, according to the authors, results in reduced variability when compared with the above models (Kim and Chung, 1992). The cuffing of the sciatic nerve model was also designed in the attempt to reduce variation in the extent of damage caused to the nerve: a standardized fixed-diameter polyethylene tube cuff is applied to the nerve, resulting in consistent levels of nerve damage, as assessed by fiber spectrum analysis (Mosconi and Kruger, 1996).

The spared nerve injury (SNI) consists of the ligation followed by axotomy of the tibial and peroneal branches of the rat sciatic nerve, leaving the sural branch intact (Decosterd and Woolf, 2000). This model results in robust physiological and behavioral changes that persist up to 6 months, with minimal variability among animals. Partial denervation allows testing of uninjured skin territories, which become hypersensitive in the result of peripheral sensitization mechanisms. The areas of the hindpaw innervated by the sural nerve and by the saphenous nerve show increased responsiveness to mechanical and thermal stimulation.

1.3. The corticostriatal circuitry

The PFC is the most rostral part of the neocortex. It is particularly important in top-down processing, coordinating a broad range of cognitive processes (Miller and Cohen, 2001). The anatomy and connectivity of the PFC are crucial for how it influences downstream brain regions. It establishes connections with all sensory and motor cortices and with several subcortical structures (Miller and Cohen, 2001). In the rodent brain, the PFC is divided in a medial region, agrannular insular and orbital regions. The mPFC is involved in several cognitive processes, including WM, decision making, attention, goal-directed behavior and inhibitory control (Heidbreder and Groenewegen, 2003). It is composed of 15% GABAergic interneurons and 85% of glutamatergic pyramidal projection neurons (Ding et al., 2001) and is divided into cyto-architectonically distinct parts along its dorsoventral axis: the medial agrannular, ACC, prelimbic (PL) and infralimbic cortices (from dorsal to ventral). The medial agrannular cortex and ACC are mainly associated with motor behaviors, having important links with the motor cortex; the infralimbic cortex is involved in visceral and autonomic activity, establishing connections with autonomic sites in the brainstem and spinal cord. In addition, the ACC has a relevant role in affective pain processing (Fuchs et al., 2014). The PL cortex is directly involved in cognitive processes, establishing important connections with the limbic system and cognition related structures (Heidbreder and Groenewegen, 2003, Vertes, 2003).

Lesions restricted to the PL cortex in rats resulted in the well described deficits in WM tasks, broadly associated with the PFC (Delatour and Gisquet-Verrier, 1996, Fritts et al., 1998, Ragozzino et al., 1998). The PL sends glutamatergic projections to structures such as the *nucleus accumbens* (NAc), the insular cortex, the amygdala, the midline thalamus (mediodorsal and reuniens nuclei) and the hippocampus are important for its role in cognitive processes. It equally receives information from these structures through both direct and indirect pathways, which are thought to converge affective, motivational, spatial and contextual information to the PL (Vertes, 2003).

The NAc is part of the basal ganglia, located in the ventral striatum. In rodents, it is segregated in a *core* region on its lateral side and a *shell* region on its ventral side, based on histochemical differences (Zahm and Brog, 1992). Recently, a fMRI study showed similar segregation of NAc areas in humans (Baliki et al., 2013). In terms of cellular composition, the NAc is constitutively composed of GABAergic medium spiny projection neurons. This nucleus is traditionally viewed as an important node in the reward circuitry, guiding behavior and directing attention towards appetitive stimuli (Floresco, 2015). Especially, it has a critical role in guiding behavior when there is ambiguity or uncertainty on what the best behavioral strategy might be to achieve a

certain goal (Floresco, 2015). The NAc is commonly considered to be an important interface between limbic and motor systems (Mogenson et al., 1993), ultimately mediating action via its output projections to motor-related areas, through the ventral pallidum and mediodorsal thalamus (Floresco, 2015).

The NAc receives important dopaminergic afferents from the midbrain, as well as glutamatergic afferents coming from cortical areas and the limbic system (Britt et al., 2012). NAc processing of incoming information is thought to bias the direction of behavior, facilitating the selection of actions that result in the best outcome. Dopaminergic projections to the NAc originate in the ventral tegmental area (VTA) and *substantia nigra* and were described to have a role influencing cortical and limbic inputs to the NAc, either amplifying or attenuating information, i.e. selecting information to be transmitted through the NAc (Mogenson et al., 1993). The hippocampus, the amygdala, and the PFC constitute perhaps the most relevant cortical and limbic projections to the NAc. These send glutamatergic projections to the NAc in a topographically organized manner, conveying information about internal motivations, context and environmental stimuli (Britt et al., 2012). The PL strongly projects to the NAc, with layer II pyramidal neurons targeting the core subregion and layer V and VI pyramidal neurons targeting both the core and shell subregions (Ding et al., 2001).

WM is one such cognitive process which seems to depend on the biasing action of the NAc. Interactions between the mPFC and the NAc are thought to subserve executive function aspects of WM, that is, the use of previously obtained information to successfully guide behavior (Kimberg and D'Esposito, 1997, Floresco et al., 1999). Consistently, several studies including lesions to the NAc or transient disconnection between the NAc and the PL-mPFC in rats, resulted in disrupted performance on different WM tasks (Seamans and Phillips, 1994, Gal et al., 1997, Floresco et al., 1999, Jongen-Relo et al., 2003). In addition, neuronal activity of the mPFC and NAc of rats coded correct/incorrect trials during a spatial delayed alternation task (Chang et al., 2002).

1.3.1. The role of the corticostriatal circuitry in pain processing

Several supraspinal brain areas are involved in pain mechanisms, both contributing to the sensory-discriminative and affective-cognitive aspects of the pain experience. The PFC was shown to be broadly activated during acute painful stimulation (Apkarian et al., 2005). Specific subregions of the PFC were associated with the processing of cognitive and affective aspects of pain. Imaging studies in humans revealed that the mPFC is activated during anticipation of pain

(Porro et al., 2002), that placebo increases activation levels of the dorsolateral and orbitofrontal cortices during anticipation of pain (Wager et al., 2004) and that the sensation of control over pain has an analgesic effect that is accompanied by increased activation of the ventrolateral PFC (Wager et al., 2004). These results highlight the fact that the unpleasantness of pain is subjective and highly modulated by emotional and cognitive aspects, such as the underlying emotional state, attention/distraction, expectations and cognitive reappraisal (Price, 2000, Bushnell et al., 2013). Importantly, the previous results are supportive of a role of the PFC in the top-down regulation and modulation of pain perception.

The NAc integrates pain information from pain processing areas, such as the PFC, amygdala, and ACC, and it was also shown to receive direct projections from the spinal dorsal horns (Burstein and Giesler, 1989, Newman et al., 1996). While pain is usually an aversive experience, pain termination or relief is rewarding, leading to phasic dopamine depressions and dopamine release in the NAc, respectively (Schultz, 2013). Importantly, conditioned place preference elicited by pain relief was shown to be associated with VTA-mediated dopamine release in the NAc, supporting a role of the NAc in mediating pain-relieving/escaping behavior (Navratilova et al., 2012). Consistently, fMRI results from humans and rats showed that pain onset is accompanied by a decrease, while pain offset is accompanied by an increase in NAc activity (Becerra and Borsook, 2008, Becerra et al., 2013). Villemure and colleagues showed that reduction of pain unpleasantness perception mediated by improved mood was positively correlated with the amount of NAc activation (Villemure et al., 2012). Furthermore, imaging studies showed the involvement of corticostriatal projections in positive reappraisal during aversive experiences, such as pain (Wager et al., 2008). Overall, the NAc is thought to be involved in signaling value and saliency of painful stimuli, ultimately promoting pain-motivated behavior and learning.

Pain chronification is accompanied by maladaptive structural plasticity in pain pathways, which is believed to underlie pain persistence and exacerbation as well as serious cognitive and affective comorbidities (Kuner and Flor, 2017). Imaging studies showed that several cortical and subcortical areas activated during acute pain stimulation are abnormally activated during chronic pain, as is the case of the PFC (Apkarian et al., 2001, Zhuo, 2008). In fact, a meta-analysis of human neuroimaging studies indicated a higher incidence of PFC activation in chronic pain as compared with experimentally induced pain (Apkarian et al., 2005). The authors speculate that this might reflect a stronger involvement of cognitive and affective components in chronic pain versus acute pain. Accordingly, prefrontal activation was more extensive during heat allodynia than during painful thermal stimulation in humans (Lorenz et al., 2002). An increase in fMRI mPFC activity was found to correlate with the intensity of pain

in patients with chronic back pain. This exacerbation was proposed to reflect the persistent negative emotional state of the patients (Baliki et al., 2006).

Electrophysiological patch clamp recordings in a neuropathic pain model showed increased intrinsic excitability of layer V ACC pyramidal neurons (Blom et al., 2014). Moreover, optogenetic stimulation of ACC inhibitory neurons resulted in a strong decrease in pain perception (Gu et al., 2015). Cordeiro Matos and Zhang analyzed layers II/III of ACC and PL mPFC regions from neuropathic pain rats and equally found increased intrinsic excitability in pyramidal neurons (Cordeiro Matos and Zhang, 2015). This was also observed in layer V neurons of the PL of neuropathic pain rats (Wu et al., 2016). However, disparate observations were reported pointing to a deactivation of PL pyramidal neurons, in spite of enhanced input glutamatergic synaptic transmission (Wang et al., 2015, Zhang et al., 2015).

A study in rats showed that during neuropathic pain, layer II/III of the PL-mPFC region undergoes severe morphological and functional changes and that there is an increase in synaptic currents of the N-methyl-D-aspartate (NMDA) component (Metz et al., 2009). The authors suggest that these changes might be related with increased glutamatergic inputs, possibly causing excitotoxicity and neuronal loss in this brain area. In fact, decreased prefrontal gray matter density was found in both humans and rats in chronic pain conditions (Apkarian et al., 2004, Seminowicz et al., 2009). Curiously, another study showed that selective infusion of a NMDA partial agonist in the PL region of the mPFC had antinociceptive properties in rats with neuropathic pain. This antinociceptive effect was proposed to result from drug-induced dissociation of relationships previously formed with spontaneous pain in the PL (Millecamps et al., 2007). This hypothesis is supportive of the idea that chronic pain is a maladaptive state of continuous learning in which aversive emotional associations are persistently made, and there is inability to extinguish them (Apkarian et al., 2009). It is further assumed that in such condition, the circuitry involved in reward/punishment learning must be in an activated state (Apkarian et al., 2009).

Lidocaine infusion in the NAc of a rat neuropathic pain model was shown to reduce neuropathic pain symptoms, revealing an important role of the NAc in the maintenance of chronic pain (Chang et al., 2014). Furthermore, a longitudinal study of a rat neuropathic pain model showed reorganization of NAc functional connectivity with different brain regions, including the mPFC, hippocampus, thalamus, sensorimotor cortices, cingulate, insula and orbitofrontal cortex (Chang et al., 2014). These changes were also accompanied by reductions in dopamine receptors (D1 and D2) expression (Chang et al., 2014). These changes are in agreement with a previous study in which the infusion of a dopamine receptor (D1 and D2) agonist diminished allodynia of neuropathic pain rats (Sarkis et al., 2011). A recent study

showed that reduced extracellular dopamine levels in the NAc during neuropathic pain leads to the disinhibition of a subset of NAc neurons related with aversive events and negative affect (indirect spiny projection neurons), which the authors showed to underlie allodynia symptoms (Ren et al., 2016). Blocking NMDA receptor activation in the NAc resulted in decreased neuropathic pain symptoms, suggesting an involvement of NAc glutamate NMDA receptor activation in the maintenance of pain symptoms (Sarkis et al., 2011). Together, these results suggest altered dopaminergic and glutamatergic activity in the NAc during chronic pain.

In humans, an imaging study showed that the NAc was differently activated in chronic back pain patients and in healthy individuals, when submitted to an acute painful thermal stimulus (Baliki et al., 2010). Interestingly, NAc functional connectivity with the mPFC was stronger in chronic back pain patients but not in healthy controls (Baliki et al., 2010). More recently, it was found that increased corticostriatal functional connectivity (between mPFC and NAc regions) could accurately predict pain chronification after a subacute back pain episode (Baliki et al., 2012).

These emerging results suggest that persistent pain acts as a persistent aversive motivation, likely engaging the corticostriatal circuitry and altering its normal functionality (Apkarian et al., 2012). Cognitive deficits associated with chronic pain conditions are broadly attributed to chronic pain-induced reorganization in the brain. In this regard, it is expected that alterations in normal corticostriatal circuitry function might impair cognitive tasks that depend on its proper functioning.

1.3.2. Optogenetic tools for manipulating specific circuits in the brain

Functional dissection of neural circuits seems to be crucial for the understanding of the neural substrates of behavior. Several approaches have been used to interfere with neural activity. Electrical manipulation of cells allows high temporal precision but greatly lacks cell-type specificity. Pharmacological and genetic approaches, on the contrary, can achieve high degrees of cell-type specificity, but without temporal precision relevant for the neural events timescale (Fenno et al., 2011). Optogenetics enables *in vivo* efficient excitation and inhibition of neurons, with high cell-type specificity and millisecond time resolution. This is achieved via illumination of light-sensitive ionic channels (“opsins”), genetically encoded in the neurons of interest. Selectively targeting a defined subset of neurons and manipulating its activity is a very useful tool to establish links between neural activity and biological functionality.

Opsins are naturally occurring light-sensitive proteins composed of 7 transmembrane helixes (Zhang et al., 2011). Upon light stimulation, these proteins are capable of transporting ions across the cell membrane. Opsins also allow the control of intracellular biochemical signaling (Pierce et al., 2002). Some of the most studied opsins are microbial (type I), and play a role in phenomena such as phototaxis, energy storage, and development, but opsins also occur in animals (type II), where they have a role in vision, in the circadian rhythm and in pigment regulation (Zhang et al., 2011). Optogenetics makes use of opsin properties to perturb target excitable cells. Opsins either act as light-activated ion pumps or as light-gated ion channels, potentially resulting in inhibition or excitation of target cells, respectively (Zhang et al., 2011).

Bacteriorhodopsins were first identified in *Halobacterium halobium* (Oesterhelt and Stoeckenius, 1971). These opsins actively transport protons from the intracellular to the extracellular space, resulting in hyperpolarization of the membrane. Other opsins act as bacteriorhodopsin-type proton-pumps, such as the proteorhodopsins and archaeorhodopsins. First found in archaebacteria, halorhodopsins (HR) pump chloride ions from the extracellular to the intracellular space, thus leading to the hyperpolarization of the membrane (Matsuno-Yagi and Mukohata, 1977). Channelrhodopsins (ChRs) act as light-gated ion channels. Channelrhodopsin-1 was identified in green algae *Chlamydomonas reinhardtii* by Nagel et al. (Nagel et al., 2002). After ChR-1, other ChRs were identified and studied. ChRs allow passive transport of cations, through a channel pore. Upon light illumination, cations flow down the electrochemical gradient, resulting in depolarization of the membrane and potentially, in an action potential.

Identification and characterization of microbial opsins was essential in the development of optogenetic tools. In 2005, Boyden et al. published the first paper on the use of opsins for fast neuronal activation. They used ChR2 to photostimulate cultured hippocampal neurons (Boyden et al., 2005). Since then, opsin genes have continuously been molecularly engineered to increase functionality and comply with different experimental design demands. The alterations aim to manipulate opsin tolerability, kinetics, spectral and trafficking properties (Carter and de Lecea, 2011). For instance, earlier ChRs were not able to evoke spike trains at frequencies higher than 40Hz, which occurs physiologically. Molecular modifications were made to accelerate channel closure kinetics, allowing accurate functioning on higher frequencies (Gunaydin et al., 2010). *Natronomonas pharaonis* HR (NpHR) when expressed in mammalian neurons has impaired subcellular localization. Second and third generation versions of NpHR (eNpHR and eNpHR3.0, respectively) have successively improved membrane trafficking, resulting in increased photocurrents and tolerability (Gradinaru et al., 2010).

Several strategies are available for targeting opsin gene expression to a given neuronal population. One of the most common methods uses viral expression systems. Infection of target cells with replication deficient virus, such as the lentivirus or the adeno-associated virus (AAV) allows high levels of opsin gene expression within a short time (2-6 weeks) and prolonged for several months, with no adverse effects (Zhang et al., 2010). Different viruses and virus pseudotypes implicate different cell tropism and transduction mechanisms. Cell-type specificity might be further improved by the choice of an adequate promoter. However, to fit in viral vectors, the promoter size is limited, which greatly reduces available cell-type specific promoters (Luo et al., 2008). Nevertheless, viral expression systems allow multiple strategies that combine genetic and anatomic specificity (Yizhar et al., 2011). For example, a specific projection might be selected if light stimulation is made in the terminal projection site, instead of in the cell soma site. Another strategy uses a recombinase-dependent system: a virus encoding Cre-recombinase is injected in the terminal projection site, and a Cre-recombinase dependent virus is injected into the cell soma site. Cells carrying Cre-recombinase dependent virus become light sensitive where they intersect the Cre-injected site (Cre moves trans-synaptically). Alternatively to using combined virus injections, Cre-dependent virus can be injected in mice endogenously expressing Cre under cell-specific promoters. This allows highly specific cell targeting and a high number of gene copies when a strong promoter is used. Opsin gene targeting might also be achieved by creating mouse transgenic lines expressing the desired opsin under the control of a cell-type specific promoter. Although this strategy is highly reliable, it is also expensive and time-consuming (Yizhar et al., 2011). *In utero* electroporation allows delivery of a high number of copies of DNA of any size, at different time points in early development. This allows precise spatiotemporal targeting of gene expression (Yizhar et al., 2011).

Photocurrents are generated upon adequate illumination of opsin-expressing cells. Light sources are most commonly lasers or LEDs. Both allow sharp spectral tuning of light, and several wavelengths matching opsin absorption peak can be obtained. Laser beams have particularly low divergence, which facilitates light focusing, important when coupling light into optical fibers, for instance. LED systems have lately been developed to also allow connection to optical fibers with greater coupling efficiencies (Clements et al., 2013). LEDs are relatively cheaper and have an easier set-up than lasers, which makes them an increasingly popular option in many experimental designs. Besides light sources, light delivery systems, as well as light propagation in the brain tissue should be considered, in order to obtain optimal light conditions in the targeted area. When targeting superficial cortical layers, LEDs can be mounted over a cranial window, leaving the tissue intact. When targeting deep areas of the

brain, optical fibers are usually used to conduct light with enough efficiency and without interfering with animal behavior. Once reaching the brain tissue, light propagates as a combination of absorption and scattering by the tissue. Light propagation is also dependent on the intensity and wavelength of the incident light, resulting in varying light spread patterns.

Light properties in the source and physical properties of the light delivery system should be precisely defined regarding optimal illumination of opsin-expressing cells. In order to achieve the desired *in vivo* effect, the light should be delivered to the opsins with the correct wavelength, intensity and temporal pattern (Mohanty and Lakshminarayananan, 2015).

1.4. Aims

Recent evidence points to an abnormal corticostriatal function during chronic pain conditions. In healthy states, the corticostriatal circuitry is broadly involved in goal-directed behavior, bridging motivations with behavioral action. There is lacking knowledge on how chronic pain interferes with normal corticostriatal function and how this might contribute to chronic pain – related cognitive deficits.

The overall aim of the present work was to investigate the role of the corticostriatal circuitry in mnemonic information processing and its impact in the manifestation of pain-related sWM deficits. In specific, the following questions were targeted:

(1) How does the corticostriatal circuit activity differently affect the performance of pre-trained and non-trained challenges of a sWM task in a neuropathic pain condition?

(2) How does the corticostriatal circuit activity affect nociceptive responses in a neuropathic pain condition?

II. Methodologies

2.1. Materials and methods

2.1.1. Animals

A total of 20 young adult male Wistar rats (weight between 250 and 350 g) were used for the experiments (Sham: *n*=10, SNI: *n*=10). Animals were purchased from the local animal facility and housed under controlled humidity (50-55%) and temperature (22-24 ºC) levels, on a 12h light/dark cycle. Throughout experiments, animals' body weight was limited to 90-95% of *ad libitum* feeding levels, with free access to water, unless otherwise stated. All animal experiments were performed in accordance with the guidelines of the European Union (2010/63/CE) and with the Research and Ethical Issues of the International Association for the Study of Pain (Zimmermann, 1983). The experimental protocols were approved by the local Ethical Committee for Animal Use and national Direção Geral de Alimentação e Veterinária board (Lisbon, Portugal).

2.1.2. Opsin gene delivery

In order to optogenetically inhibit PL-mPFC glutamatergic neurons projecting to the NAcc, HR expression was induced via injection of AAV vectors in the PL-mPFC. The virus carried a vector construct encoding the eNpHR3.0 protein and the mCherry fluorescent protein, under the human synapsin-1 (hSyn) promoter (vector construct: rAAV5/hSyn-eNpHR3.0-mCherry-WPRE, $3.0x10^{12}$ vg/mL, UNC Gene Therapy Vector Core). AAV serotype 5 has great compatibility with the nervous tissue, resulting in high levels of opsin gene expression, for prolonged periods of time, without aversive effects (Yizhar et al., 2011). Third-generation enhanced *Natronomonas* HR (variant eNpHR3.0) is an enhanced version of the *Natronomonas* HR protein (Gradinaru et al., 2010). It achieves inhibition of neurons by pumping chloride ions into the intracellular space, with high efficiency. The hSyn promoter restricts protein expression to neurons, driving strong opsin expression in both excitatory and inhibitory neurons. Moreover, this promoter allows consistent expression levels along processes, even in distant axon terminals (Diester et al., 2011).

2.1.3. Light delivery

In order to selectively stimulate PL-mPFC glutamatergic neurons projecting to the NAcc, light with a specific wavelength was delivered to the NAcc, targeting axon terminals of HR-expressing neurons.

Light was delivered through a thin optical fiber (8 mm long; 200 µm wide; 0.66 NA) implanted in the NAcc. The optical fiber was connected to an optical patch cable, which transmitted light from a LED driver (Plexon LD-1 Single Channel LED-Driver; Plexon Inc., Dallas, TX, USA). An optical commutator was used to allow free rotation of the optical patch cable, facilitating free movement of the animal during behavioral testing. A transistor-transistor logic (TTL) pulse train generator (Prizmatix Pulser 2.0, Israel) was connected to the LED driver (Plexon LD-1 Single Channel LED-Driver; Plexon Inc., Dallas, TX, USA) to control optical stimulation parameters.

Optogenetic stimulation consisted of a continuous pulse of orange LED light (λ=620 nm), with light intensity calibrated to 5 mW at the tip of the optical fiber. Light intensity was calculated to achieve a dispersion of 1 mm at the tip of the optical fiber.

2.1.4. Surgical Procedures

Virus injection, optical fiber, multi-electrode array implantation and the SNI/Sham lesion were performed in the same intervention. Rats were anesthetized with an intraperitoneal injection of a ketamine (75 mg/kg) and medetomidine (0.5 mg/kg) mixture and placed in a stereotaxic frame (David Kopf Instruments, Tujunga, CA, USA) after checking for absence of reflexes (corneal-blink and hindpaw withdrawal). Body temperature was regularly checked and maintained at 37ºC with the aid of an electric blanket. In order to prevent animals' eye drying during surgery, a lubricant was applied. During surgical procedures, 0.5 mL of saline solution was administered subcutaneously every hour.

For the stereotaxic brain surgery (Cardoso-Cruz et al., 2011), the head of the rat was shaved and cleaned with antiseptic solution (Betadine™) and a longitudinal incision was made on the skin. The skull was exposed and the muscle and connective tissue were blunt-dissected. The following coordinates relative to Bregma were used for stereotaxic targeting of PL-mPFC and NAcc structures: [PL-mPFC]: -3.2 mm anterio-posterior (AP), 0.5-0.9 medio-lateral (ML), 3.4 mm dorso-ventral (DV); [NAcc]: 1.6 AP, 0.8 ML, 7.0 DV. A craniotomy was made over the region of interest, and the *dura mater* was removed. A volume of 1 µL of virus was injected

into the PL-mPFC region. Virus was delivered at a rate of 0.1 µL/min, using a 2 µL Hamilton microsyringe (Model 7001 KH, Hamilton). After infusion, the syringe was maintained in the injection site for 5 minutes before slow removal. The optical fiber was coupled to the microelectrodes structure. The not exposed bottom portion of the optical fiber ferrule was covered with a zirconia film before assembly in the implant structure. Four screws were fixed to the skull in order to stabilize the implant and for grounding purposes. The structure was fixed with dental acrylic.

The SNI model was induced as described by the authors (Decosterd and Woolf, 2000). Briefly, a small incision was made on the skin of the rat thigh contralateral to the side of the electrodes and fiber implantation and virus injection. The *biceps femoris* muscle was blunt-dissected, exposing the three branches of the sciatic nerve. The common peroneal and tibial nerves were ligated with non-absorbent 5.0 silk in two places and a portion of the nerve (2-4 mm) was removed. The sural nerve was left intact. The control sham lesion consisted of an equal amount of skin and muscle incision, without nerve lesion.

After all the described procedures, anesthesia was reverted with subcutaneous administration of antipamezole (5.0 mg/kg). Analgesic carprofen (4.4 mg/kg) and antibiotic enrofloxacin (5.0 mg/Kg) solutions were administered subcutaneously after surgery and every 24 hours during the following 3 days. During a 7 day recovery period, the animals had free access to water and food. After surgery, each animal was housed individually until the end of the experiments.

2.1.5. Von Frey filaments test

The von Frey filaments test was used to assess the mechanical sensory threshold in the rats (Chaplan et al., 1994). The behavioral test took place in a plastic cage with a wire mesh floor (5 mm^2/square mesh), through which mechanical stimulation was performed. Each rat was allowed 15 minutes to acclimatize to the *apparatus* before testing. The rat was then tested in the mid-plantar area of the hindpaw, ipsilateral to the SNI/Sham lesion. Stimulation of the paw consisted of perpendicularly touching the hindpaw with a von Frey filament (Aesthesiometer, Somedic, SWEDEN) until it slightly bended. Each stimulus lasted for a maximum of approximately 5 seconds, or until a response occurred. Paw withdrawal, licking or flinching were considered positive responses. In the case of an ambiguous response, the stimulus was repeated. Stimulation was repeated for von Frey filaments of successively decreasing forces. Each filament was tested 10 times and the sensory threshold for noxious mechanical stimulation was determined as the force required to elicit at least 5 out of 10 positive

responses, according to the up-and-down method described by Dixon (Dixon, 1980). Mechanical sensitivity threshold was measured with and without simultaneous optogenetic stimulation. In both cases, the rat was placed in the test cage with the patch cable connected. Optical stimulation was applied during 10 seconds and filament stimulation was performed after the onset of optical stimulation. There was always a period with no optical stimulation between each filaments stimulation. The von Frey filaments test was performed at least 1 hour after DNMS probe sessions to eliminate any possible impact on cognitive performance.

2.1.6. Spatial working memory task

sWM performance was assessed with a classical DNMS task. The DNMS task was performed in a square maze (45cm x 45cm x 40cm), with two retractable levers (one in the left and one in the right) and a pellet dispenser in the center, either located in the same wall (Figure 1).

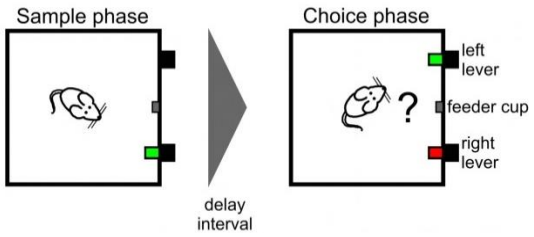

Figure 1 – Schematic representation of the DNMS task. Each trial of the DNMS task starts with the exposure of the sample lever (green). Upon sample lever press a delay period begins, in which both levers are retracted. After the delay period, the rat should choose the opposite lever (green) among the two available levers to obtain a reward.

Retractable levers position was identified by distinct visual cues (geometric figures). In the room there were also external visual cues. The position of the maze, visual cues and light intensity were maintained throughout the experiments. A trial of the task is composed of two phases: a sample phase and a choice phase, separated by a delay interval (Figure 2). Each trial is separated by an inter-trial interval (ITI) of 10 seconds. The sample phase is initiated when one of the two levers (sample) is randomly exposed (equal probability for each lever). The lever exposure is accompanied by a sound cue of 400 Hz and 400 milliseconds duration. The rat should press the presented lever within 20 seconds. Upon lever-press, the lever is retracted and a delay interval (1, 3, 6, 9, 12 or 18 seconds) is initiated. The choice phase begins in the end of the delay period with the exposure of the two levers, and this is accompanied by a second sound cue of 400 Hz and 400 milliseconds duration. The rat should press one of the two levers within 30 seconds, resulting in the retraction of both levers. A correct choice is

counted if the rat presses the opposite lever pressed during the sample phase, resulting in the delivery of a reward through the pellet dispenser – a chocolate-flavored food pellet (45 mg sucrose) (BioServ, Frenchtown, NJ, USA). If the rat fails to do the sample or the choice phases within the predicted time, exposed levers retract and an omission is signaled by a sound cue of 800 Hz and 400 milliseconds duration. The OpenControl software (adapted to this task) was used to automatically control experimental parameters and to record task events (Aguiar et al., 2007).

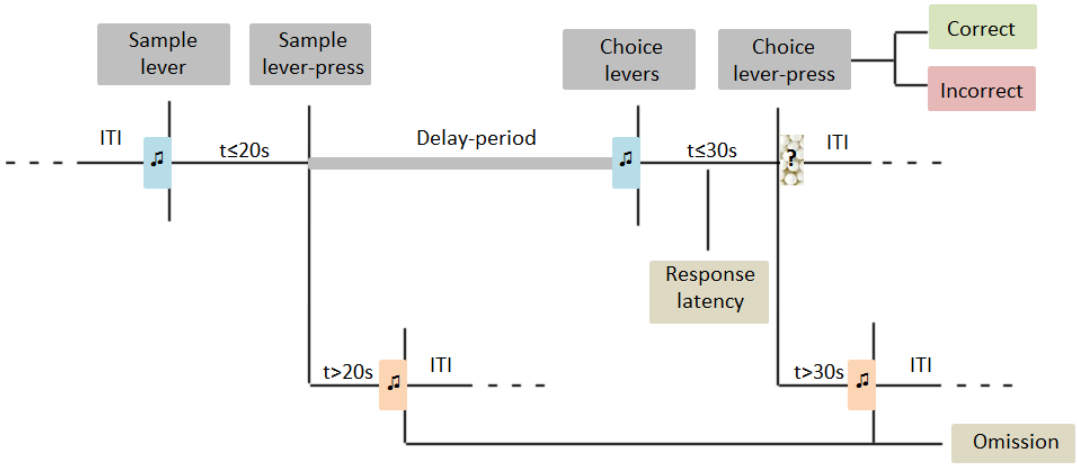

Figure 2 – Temporal organization and parameters of a DNMS task trial. Each trial of the DNMS task is preceded by an inter-trial interval (ITI). The exposure of sample and choice levers is signaled by a 400 Hz tone (blue), and the time to press these is limited to 20 and 30 seconds, respectively. If these time-intervals are exceeded, they are classified as an omission and signaled by a 800 Hz tone (orange). The correct choice lever-press is accompanied by the delivery of sucrose-pellet reward. The choice lever-press time is termed as the latency of choice response.

2.1.7. Neural recordings

The neural signals were recorded through 15 tungsten isonel-coated microelectrodes (PL-mPFC: 8, NAcc: 7) of 35 µm in diameter, with impedances varying between 0 and 0.7 MΩ at 1 kHz. The microelectrodes were connected to a wireless head-stage transmitter (W16, Triangle Biosystems), which provided wireless connection between the implanted multielectrode structure and the Multineuron Acquisition Processor system (16-MAP, PlexonInc, Dallas, TX, USA). Spiking activity and local-field potentials (LFPs) were recorded simultaneously from the same electrodes. Recorded neural signals were preamplified (10000-25000X) and digitized at 40 kHz for identification of single-unit waveforms. Neural data was sorted online (SortClient 2.6; Plexon) and validated offline (Offline Sorter 2.8; Plexon), according to five cumulative criteria (Cardoso-Cruz et al., 2011, 2013a). Extracellular LFPs were extracted by low-frequency (0.3–200 Hz) filtering of the raw signals. LFPs were preamplified and digitized at 1 kHz. A video-

tracking system (CinePlex 2, Plexon) was installed over the behavioral maze in order to record behavioral responses across experimental sessions. Video recordings and neuronal data were synchronized.

2.1.8. Histology

Histological analyses were performed in the end of the experiments, to confirm correct viral expression and optical fiber and microelectrodes location. The rats were deeply anesthetized with pentobarbital (200 mg/kg) and transcardially perfused with 0.1 M phosphate buffered saline (PBS), followed by 4% paraformaldehyde in PBS. Rat brains were dissected and post-fixed in 4% paraformaldehyde overnight at 4ºC. Rat brains were then transferred to 30% sucrose in PBS and stored at 4ºC during at least 3 days before further processing. Brain coronal slices (40 µm) were made with a freezing microtome (Leica Biosystems), washed in 0.1 M PBS and mounted on gelatinized glass slides. Alternating brain slices were stained with thionine for optical microscopy or coverslipped with mounting medium (50% glycerol in PBS) and DAPI fluorescent stain for fluorescence microscopy. Fluorescence microscopy images were obtained using a fluorescence microscope (Zeiss AxioImager.Z1) with the Apotome system (optical sectioning using structured illumination). Images were processed using the AxioVision microscope software (Apotome.2, Zeiss).

2.1.9. Experimental protocol

Animals were subjected to a pre-training period in the DNMS task (Figure 3). During this period, the rat should learn to press one of two available levers, as a mechanism to obtain a food pellet. For this, animals were put in the maze and allowed to explore during 15-minute daily sessions. Both retractable levers were exposed and pressing of any of the levers resulted in the delivery of a food pellet. The pre-training period lasted until the animal was able to press any of both levers (approximately 10-15 days of training). When this was achieved, the learning curve was initiated. The learning curve consisted of a period of training in the DNMS task with a 1-second delay interval during 10 consecutive days (one daily session of 40 trials). Only animals that achieved at least 80% of correct trials during the last 3 days of the learning curve were allowed to continue in further experiments. Animals that achieved criterion were submitted to surgery. After recovering for at least 7 days, animals were subjected to a retraining period in the DNMS task, which consisted of 5 days of training in the 1-second

DNMS challenge (one daily session of 40 trials). Probe recording sessions were initiated 4 weeks after surgeries in order to guarantee strong HR expression in the axon terminals of the infected neurons and to guarantee the stability of the SNI neuropathic pain model. Each animal was tested in the DNMS task on 5 different delay challenges: 3, 6, 9, 12 and 18-second DNMS challenges. Animals were tested on three probe sessions: after training (I) 3-second and (II) 6-second DNMS challenges; and without previous training (II) 9, 12 and 18-second DNMS challenges. Training on the 3 and 6-second DNMS challenges lasted for 6 days (one daily session of 40 trials), immediately preceding probe sessions.

Optogenetic stimulation was performed during the whole delay period (*whole*) in all DNMS challenges. Additionally for the 6-second DNMS challenges, the optical stimulation was also applied during the first half of the delay period (*early*) and during the second half of the delay interval (*late*). In control sessions no stimulation was performed (*off*). For the 3- and 6-second DNMS challenges, *off* sessions were composed of 40 trials and remaining sessions were composed of 30 trials. For the 9-, 12- and 18-second DNMS challenges, all sessions were composed of 25 trials. Animals were tested randomly on each behavioral paradigm.

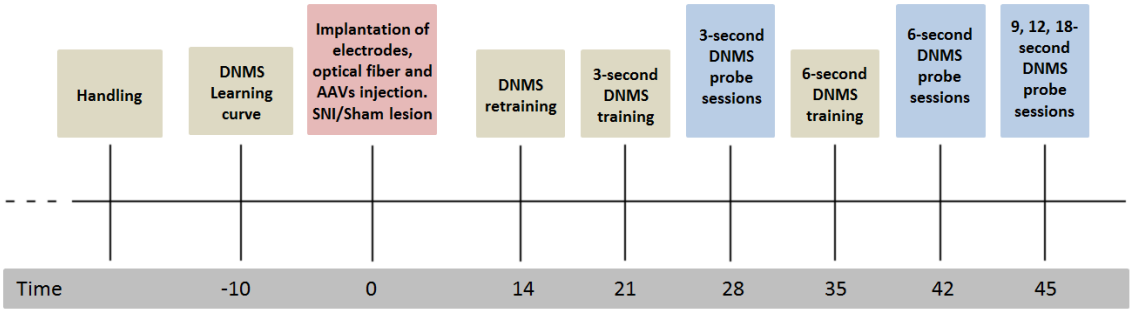

Figure 3 – **Experimental timeline.** After completing the 10 days of the DNMS learning curve, animals were submitted to surgery (day 0). After they had already recovered from surgery, they were retrained on the 1-second DNMS challenge during 5 days (aprox. day 14). They were trained in the 3-second DNMS challenge for 6 days (aprox. day 21), after which they were tested in probe sessions, when virus expression was thought to be optimal and pain levels of SNI animals were stable (aprox. day 28). They were then trained in the 6-second DNMS challenge for 6 days (aprox. day 35) and tested in probe sessions in the end (aprox. day 42). Finally, the animals were tested in the 9, 12 and 18-DNMS challenges without previous training (aprox. day 45).

2.1.10. Data analysis

Three DNMS task behavioral parameters were analysed: performance, percentage of omissions, and mean latency of choice lever response. Performance was calculated for each session as the percentage of correct trials on the total number of completed trials. Omissions were calculated for each session as the percentage of omissions on the total number of trials.

Mean latency of choice response corresponded to the time elapsed between choice levers exposure and choice lever-press, averaged per session.

Neuronal data was processed offline with NeuroExplorer 4 (NEX; Plexon), and then analysed with MATLAB (MathWorks). Population firing activity was examined during the delay period. Spiking activity data was presented as z-scores and smoothed using a Gaussian filter (3-point). To examine whether the recorded neurons exhibited task-related activity during DNMS task choice phase, the PL-mPFC firing activiy was examined around choice lever-press using perievent-time histograms (PETHs: time-window [-2, 3] sec; t=0 sec corresponds to lever-press moment; bin=50 msec). To examine reward-related activity, the NAcc firing activity was also examined around choice lever-press using PETHs (PETHs: time-window [-2, 5] sec; t=0 sec corresponds to lever-exposure moment; bin=50 msec). In perievent neuronal activity color maps, data was normalized individally across each recorded cell, and smoothed using the *fspecial* function (MATLAB native function). In PETHs, data was normalized and smoothed using a Gaussian filter (3-point). For the LFP analysis, 5 frequency bands were considered: 1-4 Hz (δ), 4-9 Hz (θ), 9-15 Hz (α), 15-30 Hz (β) and 30-50 Hz (γ). Spectral properties of PL-mPFC and NAcc LFP signals were calculated during the delay period and also during a portion of the DNMS task ITI. The power spectral density (PSD) of the LFP signals was calculated during the delay period using the fast Fourier transform analysis (FFT 512-point) (MATLAB native function) in the 0-50 Hz range of frequencies (0.19 Hz resolution). Quadratic coherence (COH2) between PL-mPFC and NAcc areas was calculated during the delay period to measure the spectral coupling of corticostriatal LFP signals, in the 0-50 Hz range of frequencies. Ranging from 0 to 1, high values of COH2 indicate great coupling of signals phases and low values indicate poor coupling of signals phases, for a given frequency (Cardoso-Cruz et al., 2013a, Cardoso-Cruz et al., 2014). Partial directed coherence (PDC) was calculated during the delay period and during the ITI (between the 3 and 7 sec) to quantify the frequency-domain connectivity between the PL-mPFC and NAcc in the 0-50 Hz range of frequencies. Also ranging from 0 to 1, high values of PDC indicate strong connectivity between recorded areas and low values indicate poor connectivity between recorded areas, for a given frequency (Cardoso-Cruz et al., 2013a, Cardoso-Cruz et al., 2014). Histograms of PSD, COH2 and PDC analysis were smoothed using a Gaussian filter (3-point).

2.1.11. Statistical analysis

The Kolmogorov-Smirnov (KS) test (with Dallal-Wilkinson-Lilliefor-corrected p-value) (Prism 6.0; GraphPad) was used to test for normality of the data. To identify differences between groups and stimulation protocols in the tested behavioral parameters (DNMS task parameters and von Frey measurements), the Kruskal-Wallis (KW) analysis of ranks test, followed by *post hoc* Dunn's tests (Prism 6.0; GraphPad) were used. The population firing distributions of experimental groups or conditions were compared using the 2-sample Kolmogorov Smirnov (KS2) test (MATLAB). For the performed spectral analyses, comparisons between experimental groups and frequency bands were based on the two-way analysis of variance (ANOVA) (group x frequency band), followed by Bonferroni *post hoc* tests (MATLAB). Comparisons between experimental groups and stimulation protocols were based on the two-way ANOVA (group x stimulation protocol). To study the correlation between PDC activity in the theta frequency band and performance in the DNMS task, the Pearson correlation test was used (MATLAB native function). The level of significance was set as 5%. Results are presented as the mean ± standard error of the mean (SEM).

III. Results

3.1. DNMS task learning curve

The DNMS task learning curve consisted of 10 sessions of the 1-second DNMS challenge. Three parameters of the task were evaluated on each session: performance, percentage of omissions and mean latency of choice response (Figure 4). Throughout the learning curve, the evaluated parameters suggested robust learning of the task rules for this challenge. Performance level increased from 59.62 % ± 3.426 on day 1 to 91.75 % ± 1.690 on day 10 (Figure 4A). The percentage of omissions decreased from 30.63 ± 5.216 on day 1 to 0.625 ± 0.4322 on day 10 (Figure 4B). The mean latency of choice response decreased from 2.89 sec ± 0.216 on day 1 to 1.17 sec ± 0.031 on day 10 (Figure 4C).

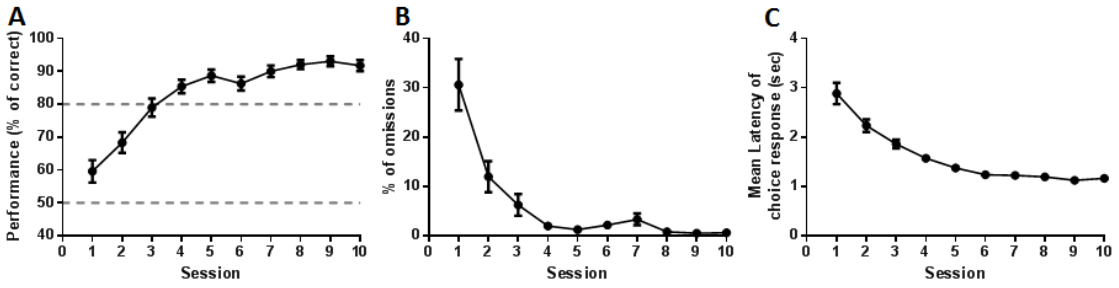

Figure 4 – **Behavioral parameters during the DNMS task learning curve. A,** Throughout the 10 days of the learning curve, performance levels increased to over 80%. **B,** The percentage of omissions per session became residual. **C,** The mean latency of choice response decreased and stabilized. Values are presented as mean ± SEM.

3.2. Halorhodopsin expression validation

Expression of eNpHR3.0 opsins was targeted to PL-mPFC glutamatergic neurons projecting to the NAcc. Optical stimulation was performed in the NAcc and neural data was recorded from the PL-mPFC and NAcc areas (Figure 5A). Specific optical stimulation of eNpHR3.0 opsins results in the active transport of chloride ions from the extracellular to the intracellular space of eNpHR3.0-expressing neurons, inhibiting its activity (Figure 5B).

In order to validate anatomically precise eNpHR3.0 expression and functional activity, histological and electrophysiological validations were performed. Histological analysis revealed a robust virus expression in cell bodies in the PL-mPFC (Figure 5C, left and upper right panels) and in neuronal processes in the NAcc (Figure 5C, lower right panel). Animals with insufficient

virus expression in the PL-mPFC and NAcc, as well as animals with incorrect optical fiber positioning were excluded from results in protocols involving optogenetic stimulation, but included in control protocols. Optical stimulation resulted in a reduction of the firing frequency of eNpHR3.0-expressing neurons, as shown by the firing activity of the representative PL-mPFC neuron illustrated, with and without optical stimulation (Figure 5D, left and right panels, respectively).

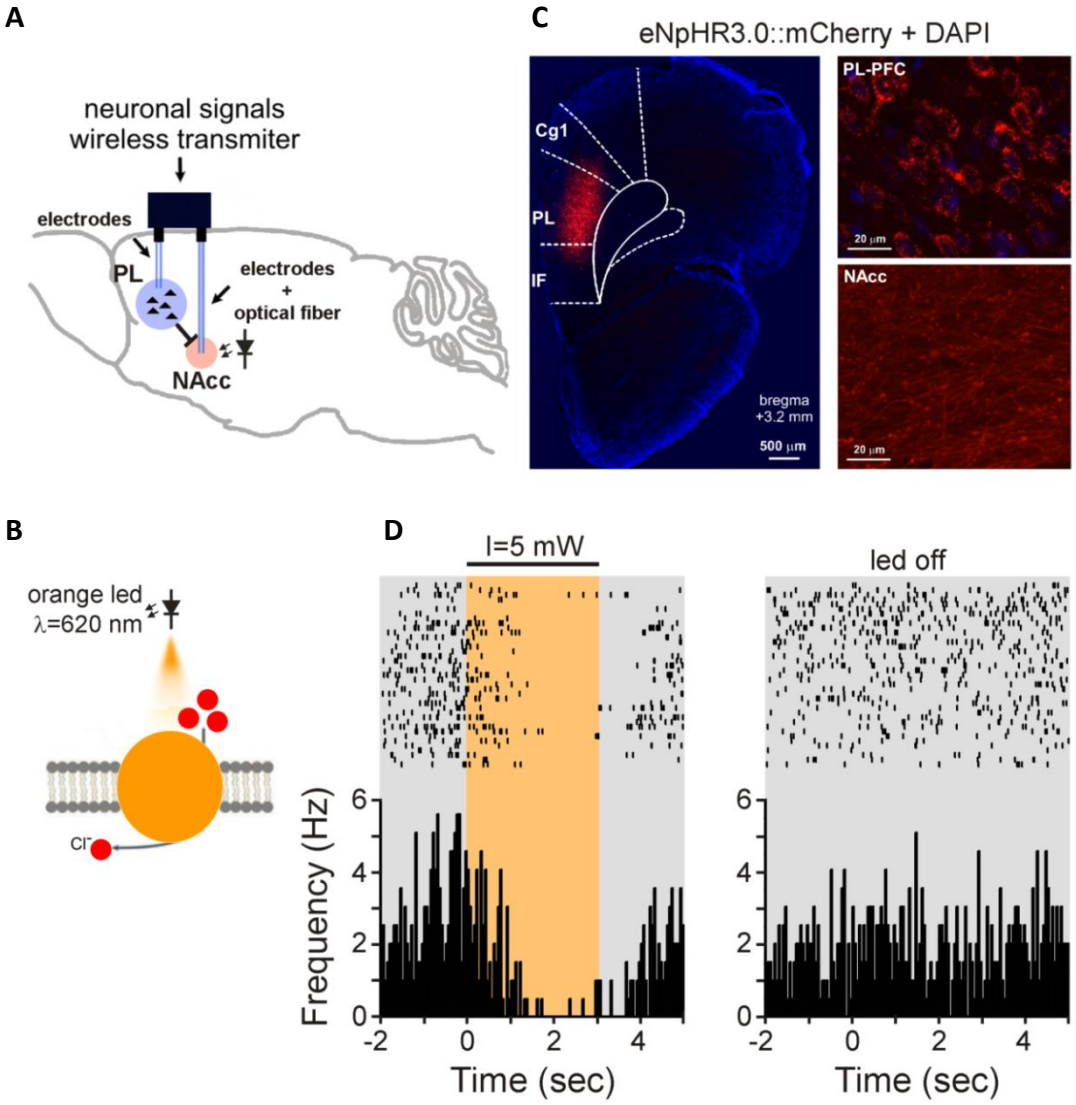

Figure 5 – Targeted corticostriatal circuit, and validation of eNpHR3.0 opsin tissue expression and function. A, Expression of eNpHR3.0 opsins was targeted to PL-mPFC glutamatergic neurons projecting to the NAcc. An optical fiber was implanted in the NAcc and microelectrodes were implanted in the PL-mPFC and NAcc. Neural signals were transmitted through a wireless transmitter. **B,** Orange LED light (λ=620 nm) stimulation of eNpHR3.0 opsins results in the transport of chloride ions from the extracellular to the intracellular space of eNpHR3.0-expressing neurons; this leads to fast hyperpolarization of the neuronal membrane, thus preventing initiation of action potentials. **C,** Histological expression of eNpHR3.0::mCherry. The left panel shows eNpHR3.0::mCherry expression in the PL-mPFC, at 3.2 mm posterior to Bregma (red: mCherry; blue: DAPI). The upper right panel shows eNpHR3.0::mCherry expression in PL-mPFC neurons soma and axon hillocks (in some neurons the axon is visible) (red: mCherry; blue: DAPI). The lower right panel shows eNpHR3.0::mCherry expression in

neuronal processes in the NAcc (red: mCherry). **D,** Firing activity of a PL-mPFC representative neuron. The photostimulation was delivered during 3 seconds with a fixed intensity of 5 mW (left histogram), and resulted in a significant decrease of spiking activity when compared to spontaneous activity without photostimulation (right histogram) (bin resolution of 100 msec).

3.3. Optogenetic modulation of the corticostriatal circuit during the delay period of pre-trained DNMS challenges

3.3.1. Effects of optogenetic modulation on working memory performance

The impact of the optogenetic modulation of the corticostriatal circuit on working memory was investigated through evaluation of the behavioral performance on pre-trained DNMS challenges: 3- and 6-second (see Materials and Methods section) (Figure 6).

The performance level of SNI animals in the 3-second DNMS challenge was slightly lower than that of Sham animals. However, statistical analysis revealed no significant differences in the performance level between experimental groups and optogenetic stimulation protocols (Figure 6A). In the case of the percentage of omissions (Figure 6B), no statistical differences were observed between experimental groups, as well as across stimulation protocols. However, it is important to note that the mean percentage of omissions decreased across the *whole* delay period stimulation protocol. In terms of response latency to choice lever-press, data showed no significant effects across experimental groups, as well as across stimulation protocols (Figure 6C).

In the case of the 6-second DNMS challenge, no significant effects were observed in the performance level between experimental groups and stimulation protocols (Figure 6D). Interestingly, SNI-treated animals showed a higher performance level when compared to control animals, specifically across the *late* delay period stimulation protocol. In addition, the SNI-treated animals revealed a higher mean percentage of omissions across all stimulation protocols (Figure 6E), but this increase was not statistically significant. In the case of response latency to choice lever-press, our data showed no significant effects across experimental groups, as well as across stimulation protocols (Figure 6F).

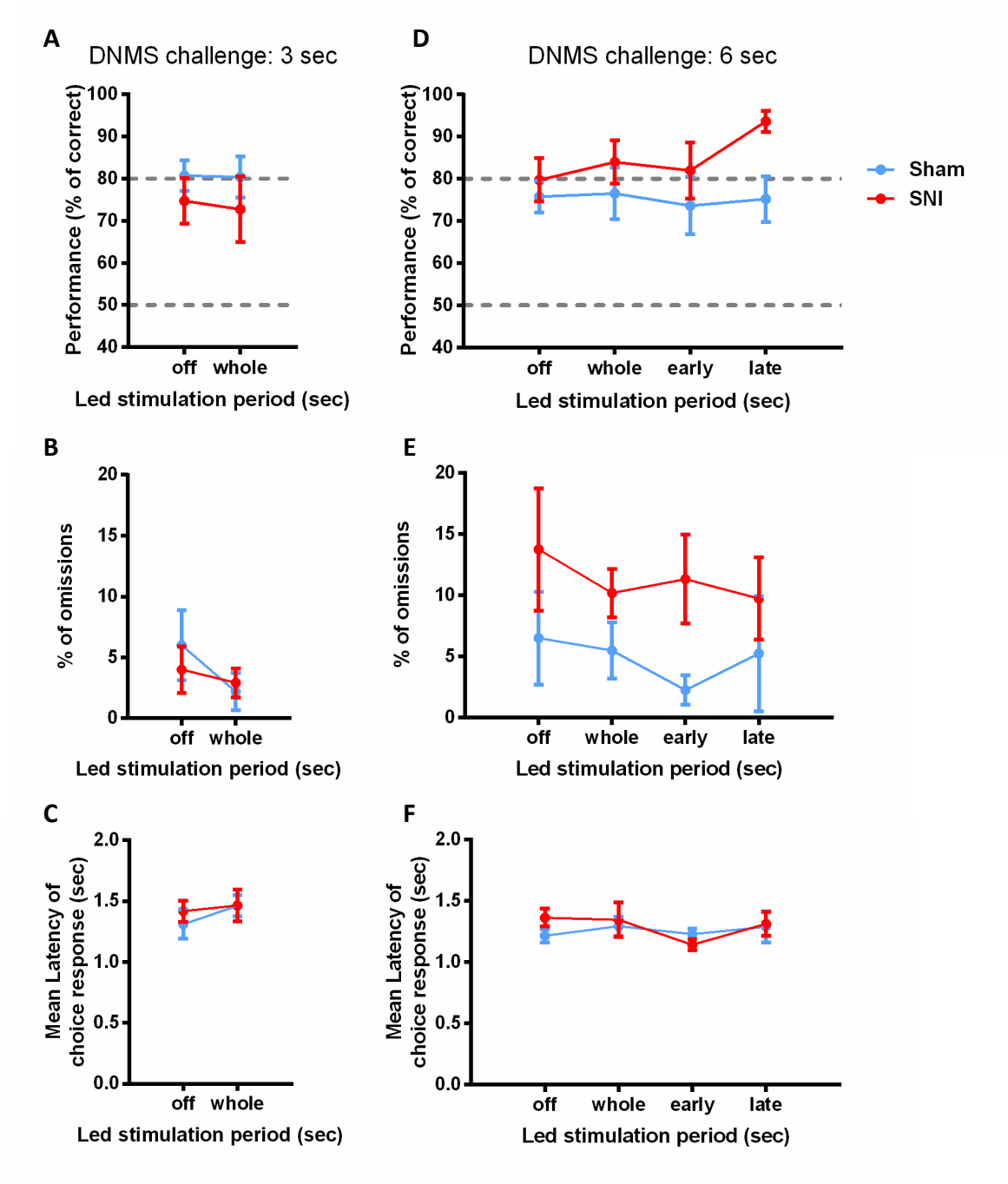

Figure 6 – Optogenetic modulation did not significantly impact behavioral performance of pre-trained 3- and 6-second DNMS challenges. Performance level **(A)**, percentage of omissions **(B)**, and mean latency of choice response **(C)** in the 3-second DNMS challenge. Performance level **(D)**, percentage of omissions **(E)**, and mean latency of choice response **(F)** in the 6-second DNMS challenge. [3-second]: *off*: Sham: *n*=10, SNI: *n*=10; *whole*: Sham: *n*=8, SNI: *n*=6; [6-second]: *off*: Sham: *n*=10, SNI: *n*=10; *whole, early* and *late*: Sham: *n*=7, SNI: *n*=6. Values are presented as mean ± SEM.

3.3.2. Effects of optogenetic modulation on corticostriatal circuit firing activity during working memory delay period

The effect of optogenetic modulation on the firing activity of PL-mPFC and NAcc recorded neurons was analyzed during the delay period of the 3- and 6-second DNMS challenges (Figure 7). It is important to note that the firing activity of both recorded areas changed its dynamics during the delay period. This occurred in both experimental groups for all tested paradigms.

The PL-mPFC population firing activity for the 3-second DNMS challenge revealed different activity patterns across both experimental groups without light delivery (*off*: KS2=0.77, *p*~0.0000, Figure 7A, left panel). Interestingly, *whole* stimulation during the delay period enhanced differences of firing activity between Sham and SNI-treated animals (KS2=0.99, *p*~0.0000, Figure 7A, right panel). In the case of the 6-second DNMS challenge, firing distributions of Sham and SNI-treated animals were significantly different in all stimulation protocols (*off*: KS2=0.56, *p*~0.0000; *whole*: KS2=0.99, *p*~0.0000; *early* :KS2=0.74, *p*~0.0000 and *late*: KS2=0.90, *p*~0.0000; Figure 7B). Similarly to the 3-second DNMS challenge, optogenetic inhibition enhanced the differences observed between experimental groups.

In relation to the NAcc population firing activity, for the 3-second DNMS challenge, no significant differences between groups were found in the *off* stimulation protocol (Figure 7C, left panel). However, significant differences were found between Sham and SNI animals in the *whole* stimulation protocol (KS2=0.99, *p*~0.0000; Figure 7C, right panel). In the 6-second DNMS challenge, significant group differences were found across all stimulation protocols (*off*: KS2=0.38, *p*~0.0002; *whole*: KS2=0.48, *p*~0.0001; *early*: KS2=0.67, *p*~0.0000 and *late*: KS2=0.74, *p*~0.0000; Figure 7D). Similarly to what happened with the PL-mPFC firing activity, optogenetic stimulation resulted in increased group differences in delay period firing activity patterns of NAcc recorded neurons.

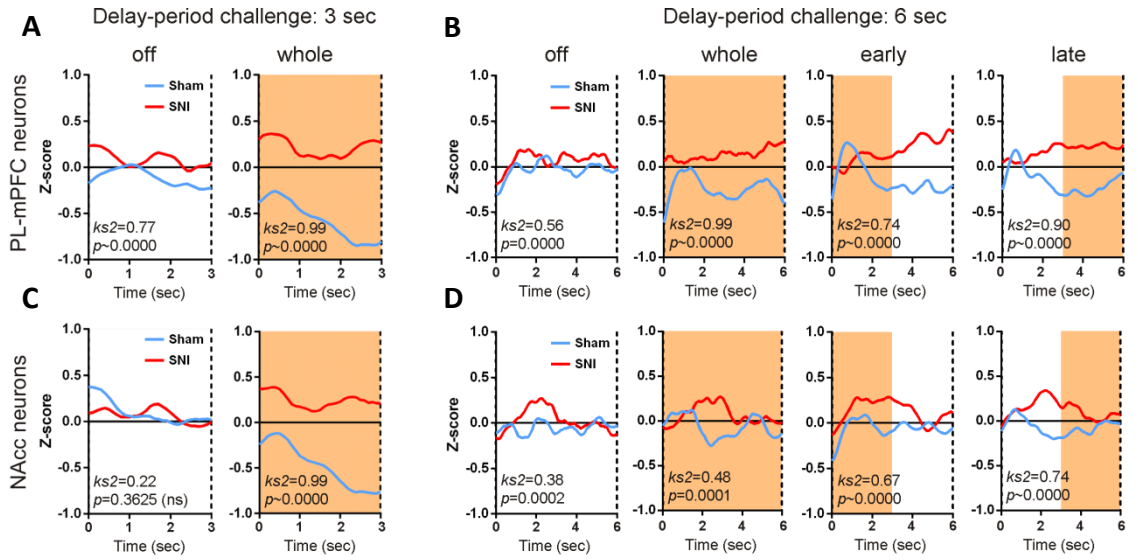

Figure 7 – Corticostriatal firing activity fluctuated during working memory delay period. Population firing activity of PL-mPFC neurons in the 3-second DNMS challenge **(A)**, and in the 6-second DNMS challenge **(B)**. Population firing activity of NAcc neurons in the 3-second DNMS challenge **(C)**, and in the 6-second delay challenge **(D)**. t=0 sec corresponds to the sample lever-press moment, when the delay period begins. Bin resolution of 50 msec. Sham: *n*=5, SNI: *n*=4. Values are presented as z-scores. Comparisons of firing distributions between experimental groups were based on KS2 test; ns="not significant".

3.3.3. Effects of optogenetic modulation on corticostriatal circuit power spectral oscillations during working memory delay period

To study the effect of optogenetic modulation on the power oscillations in corticostriatal circuit, the recorded LFP signals were analyzed during the delay period of 3- and 6-second DNMS challenges (Figure 8). Notably, the power oscillation profiles revealed that the major power differences occurred in the θ frequency band (4-9 Hz) in both recorded areas across all tested paradigms (Figure 8A).

Regarding the PSD profile of PL-mPFC LFPs in the 3-second DNMS challenge, there were no statistical differences between Sham and SNI groups. However, ANOVA revealed a significant effect, across frequency bands in both optogenetic stimulation protocols (*off*: $F_{(4,\ 35)}$=111.9, *p*<0.0001; *whole*: $F_{(4,35)}$=96.43, *p*<0.0001; Figure 8B). In the case of the 6-second DNMS challenge, statistical analysis revealed no significant differences between experimental groups, but a significant effect was observed across frequency bands, across all stimulation protocols (*off*: $F_{(4,35)}$=57.81, *p*=0.0001; *whole*: $F_{(4,35)}$=100.70, *p*<0.0001; *early*: $F_{(4,35)}$=75.45, *p*<0.0001; *late*: $F_{(4,35)}$=82.02, *p*<0.0001; Figure 8C). In addition, ANOVA revealed a significant interaction effect (groups x frequency bands factors) across *whole* and *late* stimulation protocols ($F_{(4,35)}$=5.638, *p*=0.0013; and $F_{(4,35)}$=4.31, *p*=0.0061, Figure 8C, second and fourth panels, respectively). In the

case of the *whole* delay period stimulation protocol, *post hoc* analysis revealed a higher δ power activity in Sham-treated animals when compared to SNI-treated animals ($p<0.05$), and an opposite power activity across α frequency band ($p<0.01$) (Figure 8C, second panel). In the case of *late* delay period stimulation protocol, *post hoc* analysis revealed an increase of alpha frequency band power activity in SNI-treated animals ($p<0.05$; Figure 8C, fourth panel).

In the case of the PSD profile of NAcc LFPs in the 3-second DNMS challenge, no statistical differences were found between experimental groups, but there was a significant effect across frequency bands for both stimulation protocols (*off*: $F_{(4,\ 35)}=121.1$, $p<0.0001$; *whole*: $F_{(4,35)}=145.00$, $p<0.0001$; Figure 8D). In respect to the 6-second DNMS challenge, no statistical differences between groups, but a significant effect across frequency bands was observed across all stimulation protocols (*off*: $F_{(4,35)}=222.5$, $p=0.0001$; *whole*: $F_{(4,35)}=112.4$, $p<0.0001$; *early*: $F_{(4,35)}=131.4$, $p<0.0001$; *late*: $F_{(4,35)}=124.9$, $p<0.0001$; Figure 8E). In addition, statistical analysis revealed a significant interaction effect between experimental groups, and frequency bands across the *off* and *early* stimulation protocols (*off:* $F_{(4,35)}=2.847$, $p=0.0383$; *early:* $F_{(4,35)}=3.245$, $p=0.0230$; Figure 8E, first and third panels, respectively). *Post hoc* analysis revealed an important decrease of δ power activity in SNI-treated animals when compared to control animals in the absence of light stimulation ($p<0.05$, Figure 8E, first panel).

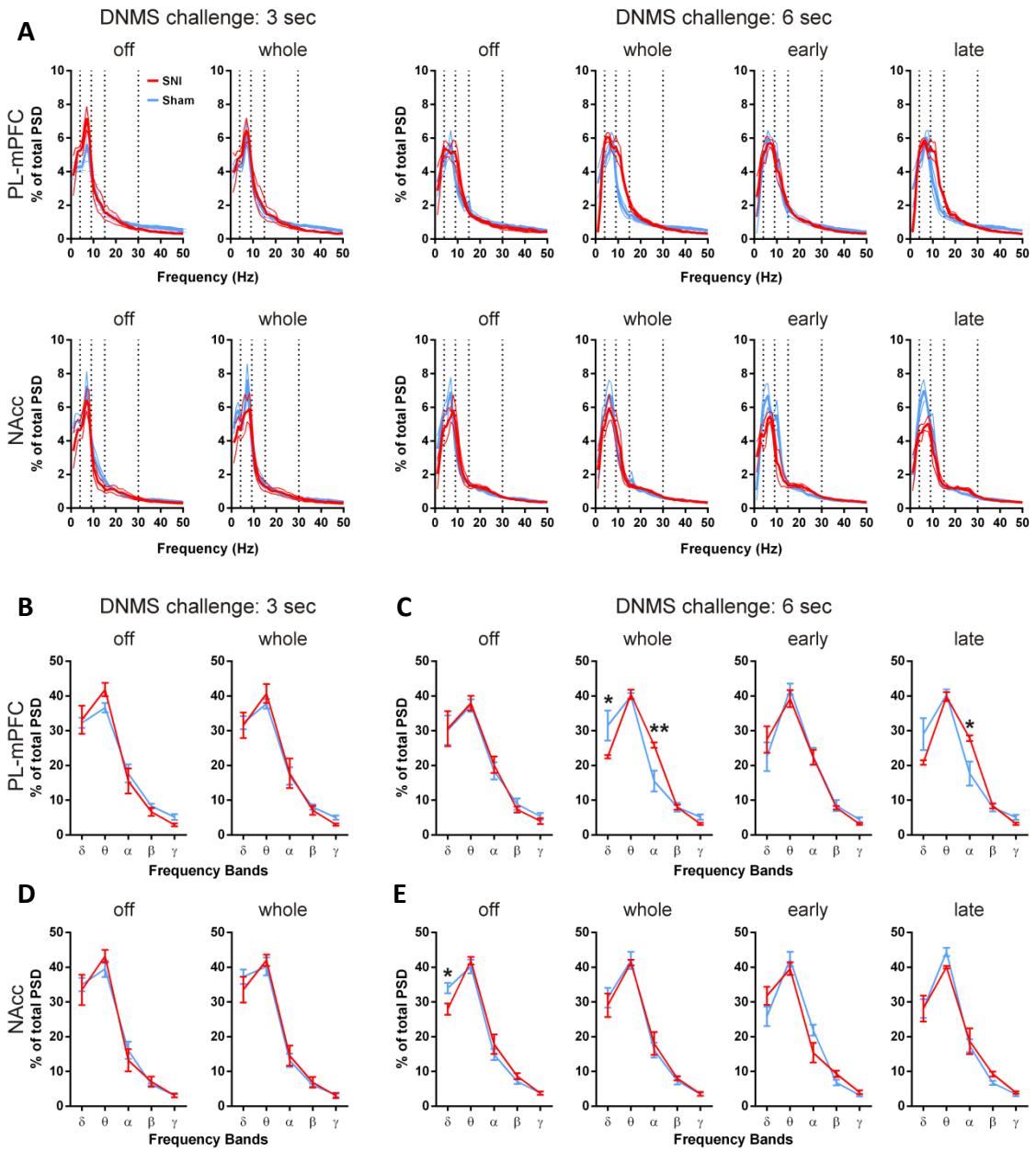

Figure 8 – Working memory delay period was characterized by predominance of θ oscillations. A, PSD profiles of PL-mPFC and NAcc LFPs activity in the 3- and 6-second DNMS challenges show a predominance of θ frequency band power in both recorded areas and experimental groups, across all tested paradigms (bin resolution of 1 Hz). **B, C,** PSD profiles of PL-mPFC LFPs activity per frequency band show similar patterns for Sham and SNI animals in the majority of tested paradigms. The exception was observed for the 6-second DNMS challenge in α-band with a power increase for *whole* and *late* protocols, and in δ-band with a decrease for the *whole* protocol in SNI-treated animals **(C)**. **D, E,** PSD profiles of NAcc LFPs activity per frequency band also indicate similar activity between experimental groups and stimulation protocols, except for a decrease of δ power activity in the *off* stimulation protocol for SNI-treated animals in the 6-second DNMS challenge **(E)**. Sham: n=5, SNI: n=4. Values are presented as mean ± SEM. Comparisons between experimental groups and frequency bands were based on the two-way ANOVA (group x frequency band), followed by *post hoc* Bonferroni test. *p<0.05; **p<0.01.

3.3.4. Effects of optogenetic modulation on corticostriatal circuit spectral coherence oscillations during working memory delay period

The effect of photostimulation in the corticostriatal circuit coherence activity of eNpHR3.0-expressing rats is illustrated in Figure 9. A strong COH2 activity was observed across the θ frequency band for all tested paradigms (Figure 9A). In the case of the 3-second DNMS challenge, ANOVA revealed no significant differences between experimental groups and frequency bands (Figure 9B). In the case of the 6-second DNMS challenge, no statistical differences were found between experimental groups, but there were statistical differences between frequency bands (*off*: $F_{(4,\ 35)}$=10.49, p<0.0001; *whole*: $F_{(4,35)}$=6.282, p=0.0006; *early*: $F_{(4,35)}$=11.28, p<0.0001; *late*: $F_{(4,35)}$=9.612, p<0.0001; Figure 9C).

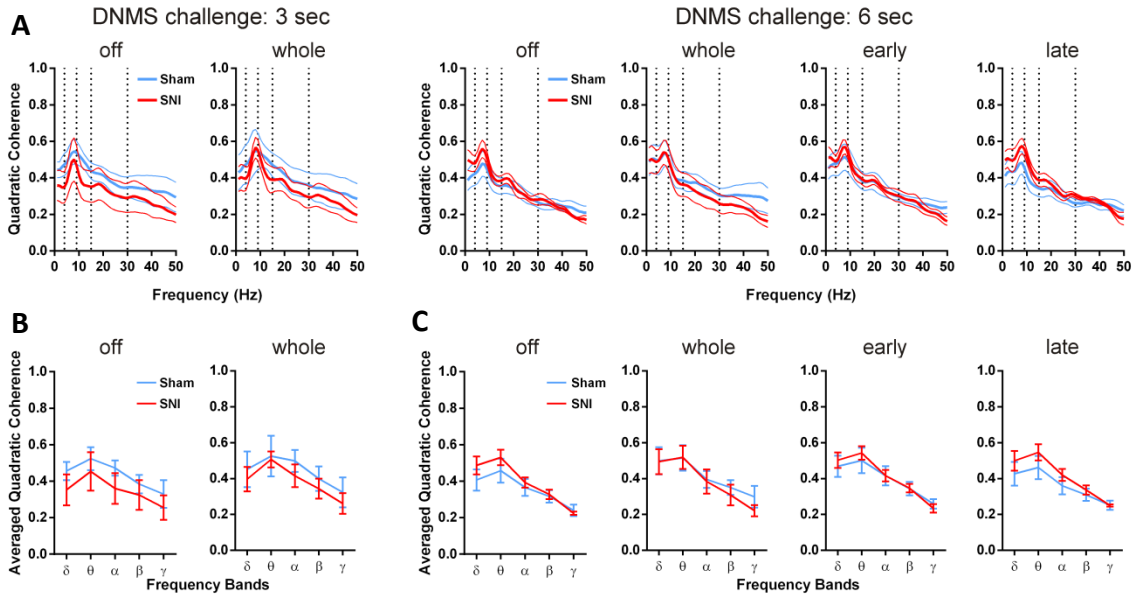

Figure 9 – Corticostriatal coherence was higher in the θ frequency band during working memory delay period. A, Traces of COH2 in the corticostriatal circuit (bin resolution of 1 Hz). **B, C,** Corticostriatal COH2 per frequency band of Sham and SNI animals was not significantly different in any tested paradigm. Sham: *n*=5, SNI: *n*=4. Values are presented as mean ± SEM.

3.3.5. Effects of optogenetic modulation on corticostriatal connectivity during working memory delay period

To study the effect of optogenetic modulation on the corticostriatal connectivity, PDC activity was analyzed during the delay period of 3- and 6-second DNMS challenges (Figure 10). PDC activity values clearly showed a peak in the corticostriatal connectivity in the θ frequency band, indicating an increase of information processed across this frequency band (Figure 10A). Considering this result, averaged values of PDC activity in the θ frequency band were considered to further analysis.

In the 3-second DNMS challenge, ANOVA revealed no significant differences in θ PDC activity between experimental groups and stimulation protocols (Figure 10B). In the case of the 6-second DNMS challenge, no significant differences were found in the PL-mPFC>>NAcc direction between experimental groups and stimulation protocols (Figure 10C, left panel). However, a significant effect was observed between experimental groups and stimulation protocols in the NAcc>>PL-mPFC direction (group: $F_{(1,14)}$=4.346, p=0.0463, stimulation protocol: $F_{(1,14)}$=3.060, p=0.0444; Figure 10C, right panel). Moreover, *post hoc* tests revealed a higher NAcc>>PL-mPFC PDC activity for SNI–treated animals in the absence of optical stimulation (p<0.01; Figure 10C, right panel).

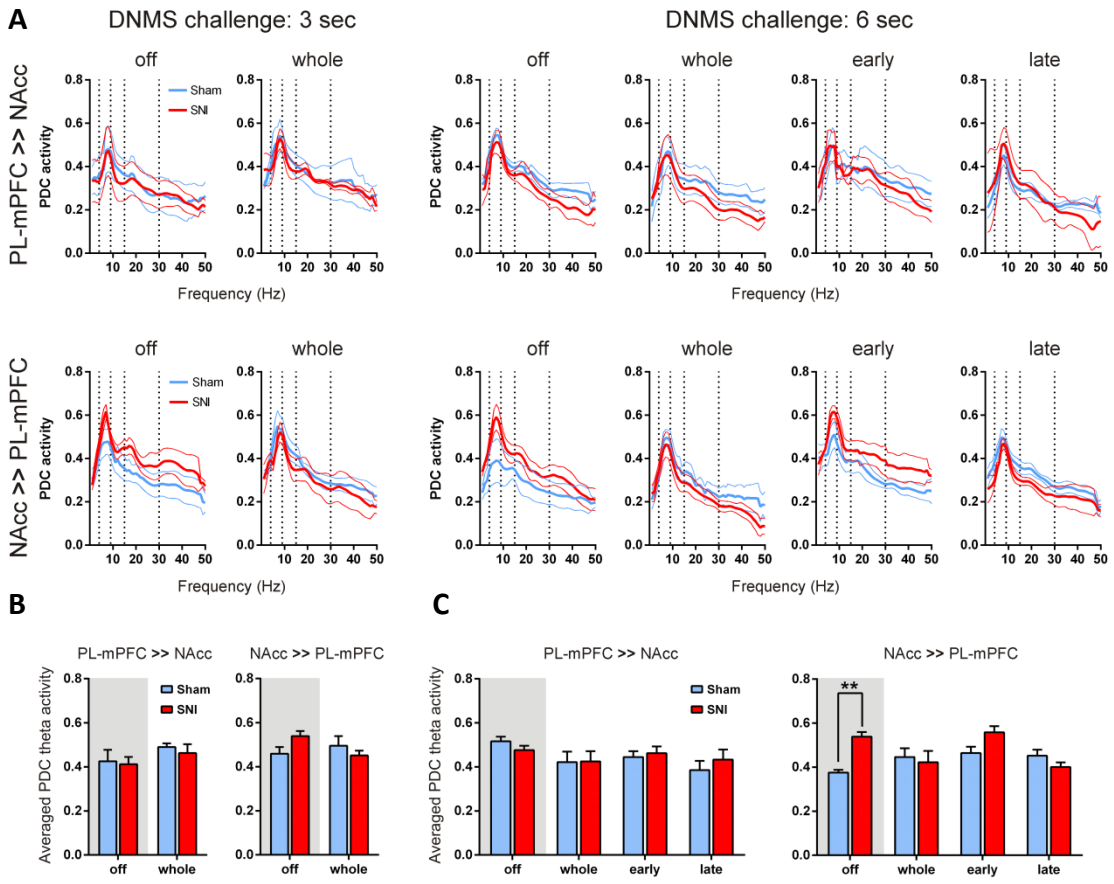

Figure 10 – SNI-treated animals increased their NAcc>>PL-mPFC connectivity during working memory delay period. A, Bidirectional PDC activity in the 3- and 6-second DNMS challenges (bin resolution of 1 Hz). In all paradigms, there was a peak of PDC values in the θ frequency band. **B, C,** Analysis of bidirectional PDC activity in the θ frequency band in the 3-second **(B)** and in the 6-second DNMS challenge **(C)**. SNI-treated animals presented a higher θ frequency band NAcc>>PL-mPFC direction connectivity, in the absence of light delivery across the 6-second DNMS challenge. Sham: *n*=5, SNI: *n*=4. Values are presented as mean ± SEM. Comparisons between groups and frequency bands were based on the two-way ANOVA (group x frequency band), followed by post-hoc Bonferroni test. ***p*<0.01.

3.3.6. Correlation between corticostriatal connectivity and working memory performance

To determine whether corticostriatal θ frequency band connectivity was modulated by behavioral flexibility required for correct decision-making processes, a correlation between the level of corticostriatal PDC θ frequency connectivity during the delay period and DNMS performance level was performed. The present data showed that, globally, an increase of the performance level is accompanied by an increase of the corticostriatal circuit connectivity level in both circuit directions (Figure 11).

The PL-mPFC>>NAcc direction connectivity in θ-band was positively correlated with the performance level of both experimental groups across the 3-second DNMS challenge. ([*off*]*:* Sham: R^2=0.8945, *p*=0.0150; SNI: R^2=0.9178, *p*=0.0420; [*whole*]: Sham: R^2=0.8945, *p*=0.0150; SNI: R^2=0.9178, *p*=0.0420; Figure 11A, left and right panels, respectively). In the case of the 6-second DNMS challenge without optical stimulation, a significant positive correlation was observed in both experimental groups (Sham: R^2=0.8901, *p*=0.0160; SNI: R^2=0.9328, *p*=0.0342, Figure 11B, first panel). No significant correlations between PL-mPFC>>NAcc connectivity and performance were encountered in the remaining stimulation protocols. In ascending circuit direction, from NAcc to PL-mPFC, in the 3-second DNMS challenge, the data showed only a significant positive correlation between PDC activity and performance in SNI-treated animals across the *whole* delay period stimulation (R^2=0.9451, *p*=0.0278, Figure 11C, right panel). For the 6-second DNMS challenge, significant positive correlations were found for Sham animals in the *whole* and *early* stimulation protocols (*whole*: R^2=0.9473, *p*=0.0267; *early*: R^2=0.9674, *p*=0.0165, Figure 11D, second and third panels, respectively).

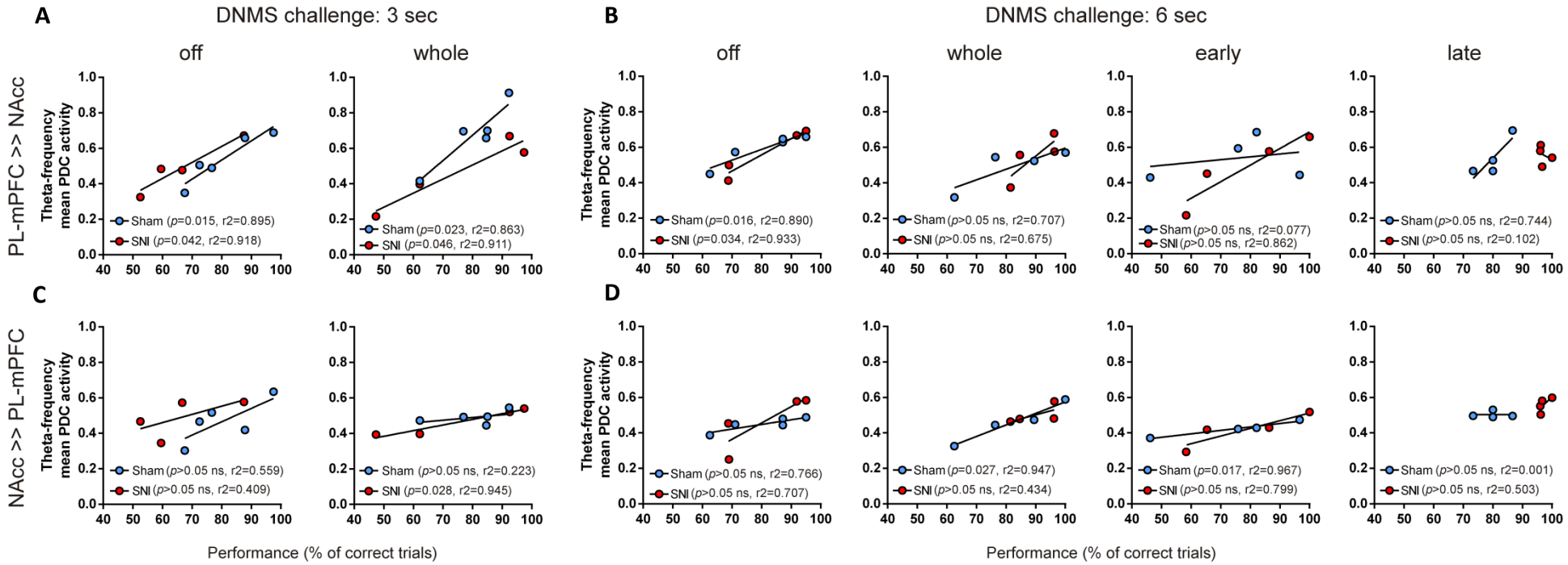

Figure 11– Theta corticostriatal connectivity is positively correlated with working memory performance. A, B, Correlation between averaged PDC activiy in the θ frequency band in the PL-mPFC>>NAcc direction and performance levels in the 3-second **(A)**, and in the 6-second DNMS challenge **(B)**. Significant positive correlations were found for both Sham and SNI groups in both stimulation protocols of the 3-second DNMS challenge and in the *off* stimulation protocol of the 6-second DNMS challenge **C, D,** Correlation between averaged PDC values in the θ frequency band in the NAcc>>PL-mPFC direction and performance levels for the 3-second DNMS challenge **(C)**, and for the 6-second DNMS challenge **(D)**. Significant positive correlations were found for the SNI group in the *whole* stimulation protocols of the 3-second DNMS challenge, and for the Sham group in the *whole* and *early* stimulation protocols of the 6-second DNMS challenge. Sham: *n*=5, SNI: *n*=4. Correlation analysis between PDC and performance values was based on the nonparametric Pearson coefficient test.

3.3.7. PL-mPFC firing activity during working memory decision-making

To evaluate whether PL-mPFC firing activity was affected by the moment of decision between two alternative levers in the DNMS task, PL-mPFC population firing activity was analyzed around the choice lever-press moment (Figure 12).

Interestingly, both Sham and SNI neurons showed a consistent elevation of firing activity in the moment that precedes the lever-press (t=0 sec). This effect was observed in *off*, as well as in *on* (here referring to *whole* and *late*) stimulation protocols (Figure 12A). An example of two illustrative neurons is given in Figure 12B. In terms of PL-mPFC population activity, both experimental groups showed different firing distributions in the absence or in the presence of light delivery (*off*: KS2=0.24, $p<0.0050$; *on*: KS2=0.27, $p<0.0010$; Figure 12C). Notably, SNI neurons had increased firing activity, when compared to control neurons. Finally, and as expected, optogenetic stimulation (*on*) resulted in a decrease in the frequency of firing of both Sham and SNI neurons, when compared with no stimulation (*off*) (Sham: KS2=0.29, $p\sim0.0000$; SNI: KS2=0.37, $p\sim0.0000$; Figure 12D).

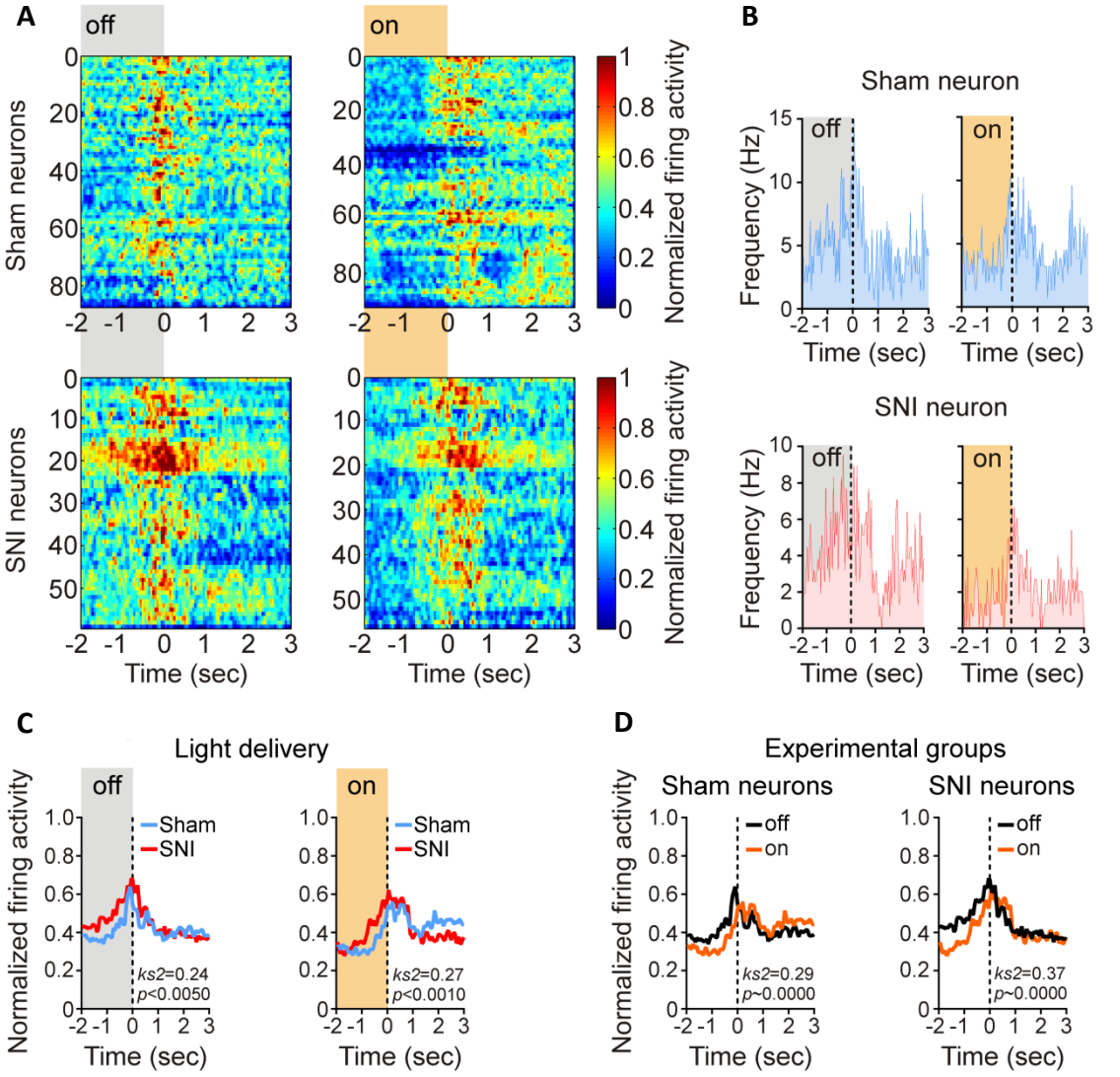

Figure 12 – PL-mPFC firing activity was increased during working memory decision-making. A, Perievent neuronal activity color maps of Sham and SNI neurons, in *off* and *on* stimulation protocols (bin resolution of 50 msec). A marked increase of spiking activity was observed around the choice lever-press moment for both experimental groups (t=0 sec corresponds with the choice lever-press moment). **B,** Perievent time histograms of a representative Sham and SNI neuron, in the absence and in the present of light stimulation (bin resolution of 50 msec). **C, D,** Population firing activity of Sham and SNI groups, in *off* and *on* stimulation protocols (bin resolution of 100 msec). Data for this analysis were collected from both 3- and 6-second DNMS challenge sessions, indiscriminately. Sham: *n*=5, SNI: *n*=4. Comparisons of firing distributions between experimental groups were based on the KS2 test.

3.3.8. NAcc neuronal activity across correct and incorrect trials

To examine whether NAcc firing activity differently encoded correct and incorrect trials, NAcc population firing activity was analyzed around choice lever response (Figure 13).

The NAcc population firing activity was strikingly different across correct and incorrect trials (Figure 13A). During correct trials, both Sham and SNI neurons exhibited elevated firing activity before choice levers-press, which decreased after response (Figure 13B, left panel). In contrast,

during incorrect trials, firing activity was decreased before choice levers-press and increased after response (Figure 13B, right panel). Although showing the same above described pattern, Sham and SNI groups were shown to have statistically different firing activity distributions in correct trials (KS2=0.3143, *p*~0.0000; Figure 13B, left panel). For incorrect trials, no significant differences were found between experimental groups (Figure 13B, right panel). Figure 13C illustrates the firing activity of two representative neurons across correct and incorrect trials.

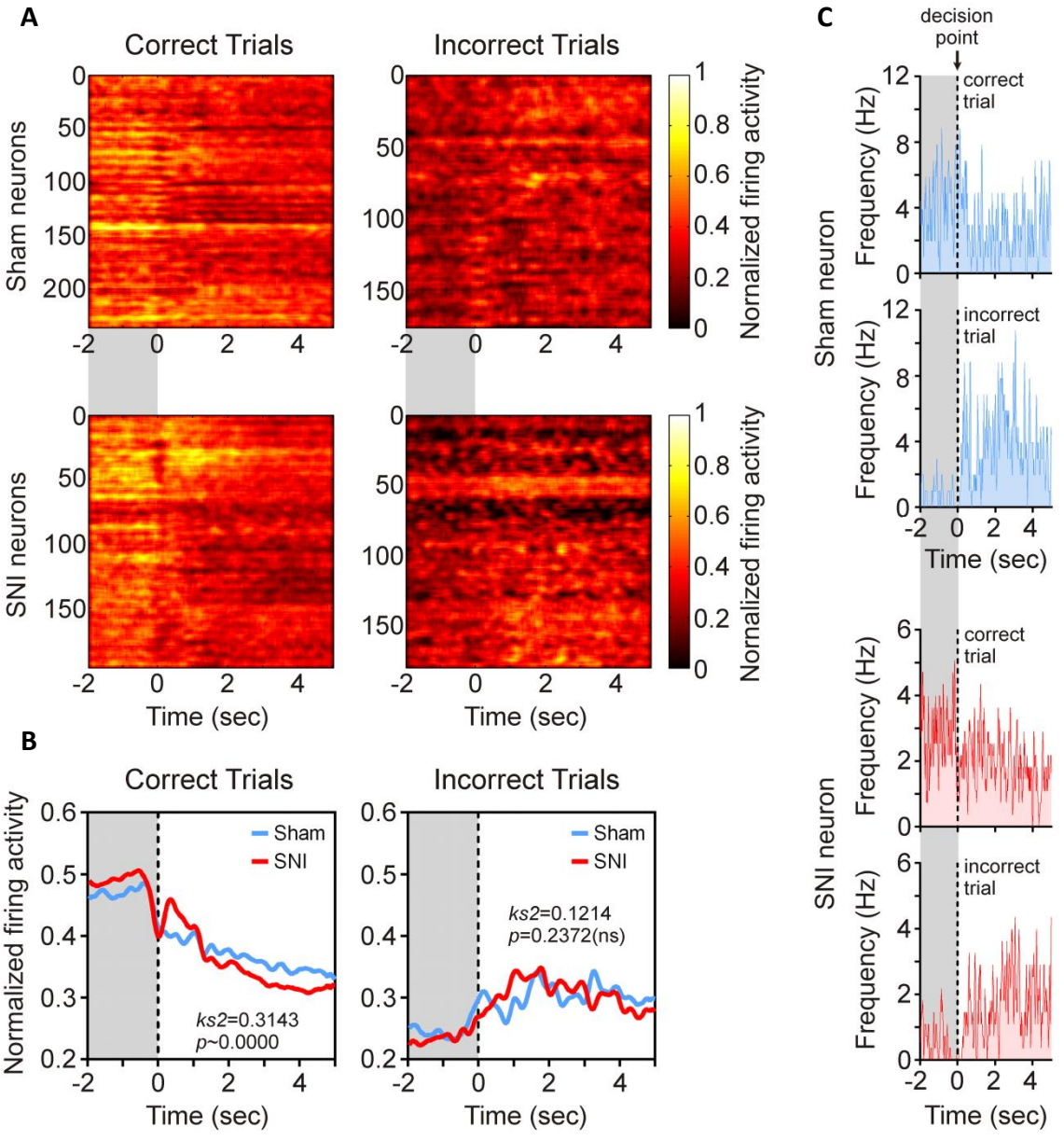

Figure 13 – NAcc revealed different reward-related activity across correct and incorrect trials. A, Perievent neuronal activity color maps of Sham and SNI neurons across correct and incorrect trials (bin resolution of 50 msec). During correct trials, recorded neurons increased their activity before choice lever-press (t=0 corresponds with the choice lever exposure moment). An opposite effect was observed during incorrect trials. **B,** NAcc population firing activity of Sham and SNI groups across correct and incorrect trials (bin resolution of 100 msec). Correct trials were associated with a decrease in firing activity, while incorrect trials were associated with an increase in firing activity. **C,** Perievent time

histograms of a representative Sham and SNI neuron across correct and incorrect trials (bin resolution of 50 msec). Comparisons of firing distributions between experimental groups were based on the KS2 test; ns="not significant". Sham: *n*=5, SNI: *n*=4. Data for this analysis were collected from both 3- and 6-second DNMS challenge sessions, indiscriminately.

3.4. Optogenetic modulation of the corticostriatal circuit during the delay period of non-trained DNMS challenges with increased complexity

3.4.1. Effects of optogenetic modulation on working memory performance

The impact of the optogenetic modulation of the corticostriatal circuit on working memory was further investigated through evaluation of the behavioral performance on non-trained DNMS challenges with higher delay periods: 9-, 12-, and 18-second (see Materials and Methods section) (Figure 14). Overall, optogenetic stimulation resulted in an improved performance level of SNI-treated animals, but did not have an impact in control animals (Figure 14A and 14B). In addition, both experimental groups revealed an increase in the latency response to choice lever-press when compared to low-complexity trained DNMS challenges (Figure 14C and 14D), but no significant oscillations were observed in the percentage of performed omissions (Figure 14E and 14F).

Statistical analysis revealed a significant delay-dependent decrease of performance level across both experimental groups in the absence of light stimulation, which is a hallmark of WM tasks (*off*: KW=31.84, *p*=0.0002; Figure 14A, left panel). For the *whole* delay period stimulation protocol, significant differences were observed between groups and DNMS challenges (KW=20.46, *p*=0.0153; Figure 14A, right panel). *Post hoc* analysis revealed a higher performance level of SNI-treated animals in the 18-second DNMS challenge when compared to controls (*p*<0.05; Figure 14A, right panel).

For Sham-treated animals, intra-group analysis showed a significant effect across DNMS challenges (KW=23.77, *p*=0.0047; Figure 14B, left panel), but not across stimulation protocols. In relation to SNI-treated animals, statistical analysis revealed a significant effect across stimulation protocols (KW=23.77, *p*=0.0047; Figure 14B, right panel). *Post hoc* analysis revealed that optogenetic inhibition of eNpHR3.0-expresing SNI-treated animals significantly increased their working memory performance for 9- and 18-second DNMS challenges (*p*<0.05, and *p*<0.01, respectively; Figure 14B, right panel).

In respect to the mean latency of choice response, statistical analysis revealed no significant differences between experimental groups when tested in the absence of light stimulation or

with *whole* delay period stimulation. However, there was a significant effect of the delay period length across both stimulation protocols (*off*: KW=53.40, $p<0.0001$, and *whole*: KW=26.94, $p<0.0014$, Figure 14C). Intra-group statistical analysis of Sham and SNI-treated animals indicated no significant differences between stimulation protocols, but a significant effect of the delay period length was visible across both experimental groups (Sham: KW=42.96, $p<0.0001$; SNI: KW=37.46, $p<0.0001$; Figure 14D). Overall, the mean latency of choice response was similarly low in the 3- and 6-DNMS challenges and higher for more complex DNMS challenges. Interestingly, mean latency of choice response levels in the 9-, 12-, and 18-second DNMS challenges decreased with increasing length of the delay period (Figure 14C and 14D).

Statistical analysis of the percentage of omissions revealed no significant differences between experimental groups when tested in the *off* or in the *whole* delay period stimulation (Figure 14E). Moreover, intra-group comparisons revealed no significant differences between stimulation protocols (Figure 14F).

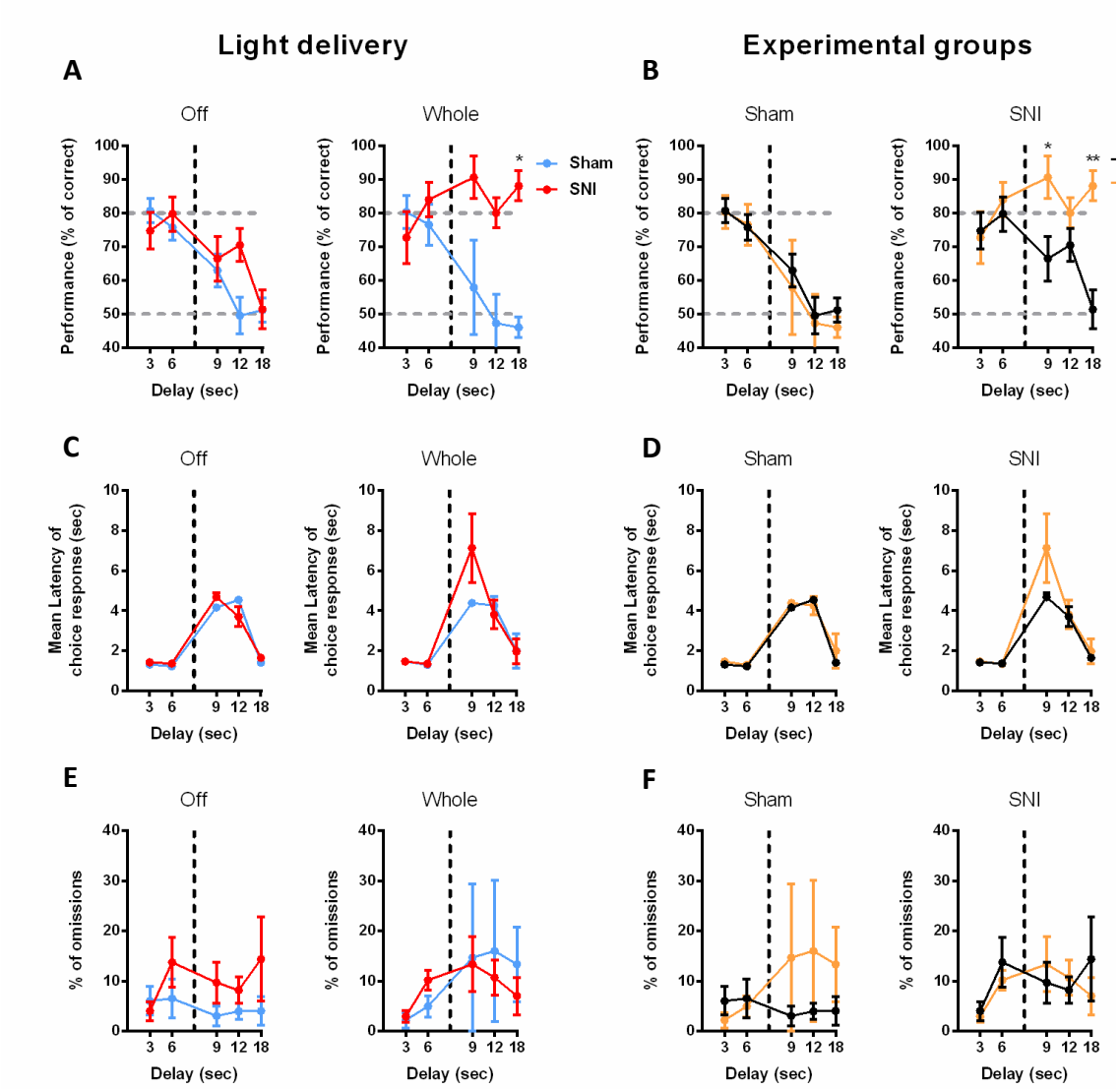

Figure 14 – Optogenetic stimulation improved SNI but not Sham performance level in non-trained DNMS challenges A, B, Performance levels of Sham and SNI groups in 3-, 6-, 9-, 12- and 18-second DNMS challenges, per stimulation protocol **(A)** and per experimental group **(B)**. Optical stimulation during the delay period resulted in significantly improved performance levels in SNI-treated animals in the 9- and 18-second DNMS challenges, but did not impact performance level of Sham-treated animals. **C, D,** Mean latency of choice response of Sham and SNI groups in 3-, 6-, 9-, 12- and 18-second DNMS challenges. There was an effect of the delay period length on the mean latency of choice response, across all paradigms. **E, F,** Percentage of omissions per session of Sham and SNI groups in 3-, 6-, 9-, 12- and 18-second DNMS challenges. [3- and 6-seconds]: *off*: Sham: *n*=10, SNI: *n*=10; *whole:* Sham: *n*=8, SNI: *n*=6; [9- and 18- seconds]: *off*: Sham: *n*= 4, SNI: *n*=9; *whole:* Sham: *n*=3, SNI: *n*=5; [12-seconds]: *off*: Sham: *n*=10, SNI: *n*=9; *whole*: Sham: *n*=3, SNI: *n*=5. Values are presented as mean ± SEM. Comparisons between experimental groups and stimulation protocols were based on the KW test (3- and 6-second DNMS challenges were included), followed by Dunn's *post hoc* test. *p<0.05; **p<0.01.

3.5. Effects of the optogenetic modulation of the corticostriatal circuit on nociception

Mechanical sensory threshold values were measured with the von Frey filaments test (Figure 15). Measurements were performed at least one hour after DNMS task probe sessions. The effects of optogenetic modulation of PL-mPFC excitatory neurons were tested applying an inhibitory pulse of 5 mW and in the absence of light stimulation. Statistical analysis revealed significant differences in the mechanical sensory threshold between experimental groups (KW=25.78, p<0.0001). *Post hoc* analysis showed that the pressure needed to evoke a response was lower in the SNI group when compared to the Sham group (light *off*: Sham vs. SNI, p<0.001; and light *on*: Sham vs. SNI, p<0.05; Figure 15). Moreover, no significant optogenetic stimulation effects were observed in intra-group comparisons (Sham: light *off* vs. *on*, n.s.; and SNI: light *off* vs. *on*, n.s.).

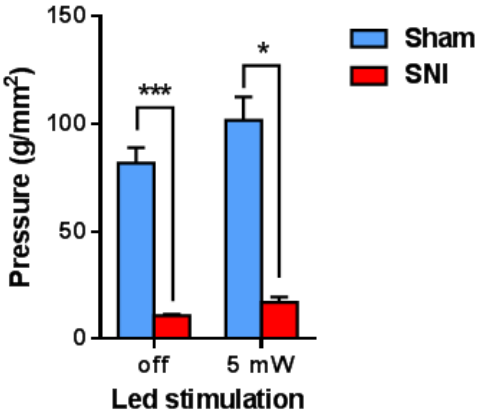

Figure 15 – Corticostriatal circuit selective inhibition did not produce antinociceptive effects. Mechanical sensory threshold was measured with the von Frey filaments test. SNI-treated animals were significantly more responsive to von Frey filament stimulation than control animals, independently of optogenetic stimulation. In fact, optical stimulation did not induce significant differences in the mechanical sensory threshold of Sham and SNI-treated animals. [off]: Sham: n=10, SNI: n=10; [5 mW]: Sham: n=7, SNI: n=5. Values are presented as mean ± SEM. Comparisons between experimental groups and stimulation protocols were based on the KW test, followed by Dunn's post hoc test. *p<0.05; ***p<0.001.

3.6. Changes in corticostriatal connectivity induced by the SNI model of neuropathic pain

To examine alterations of spontaneous corticostriatal connectivity oscillations across experimental groups, the PDC activity was analyzed during a portion of the ITI period of the DNMS task (Figure 16B). This portion of time is thought to be relatively less affected by task-related activity.

Similarly to the PDC activity profile observed during the delay period, PDC activity also had a strong θ frequency band component (Figure 16A). In the case of the PL-mPFC>>NAcc direction, ANOVA revealed significant differences between experimental groups and frequency bands

($F_{(1,35)}$=15,50, p=0.0004, and $F_{(4,35)}$=72.94, p<0.0001, respectively). *Post hoc* analysis specifically revealed that PDC activity in the α frequency band was increased in SNI-treated animals when compared with control animals (p<0.05, Figure 16C, upper panel). In the NAcc>>PL-mPFC direction, differences were found between frequency bands but not across experimental groups ($F_{(4,35)}$=58.66, p<0.0001; Figure 16C, lower panel).

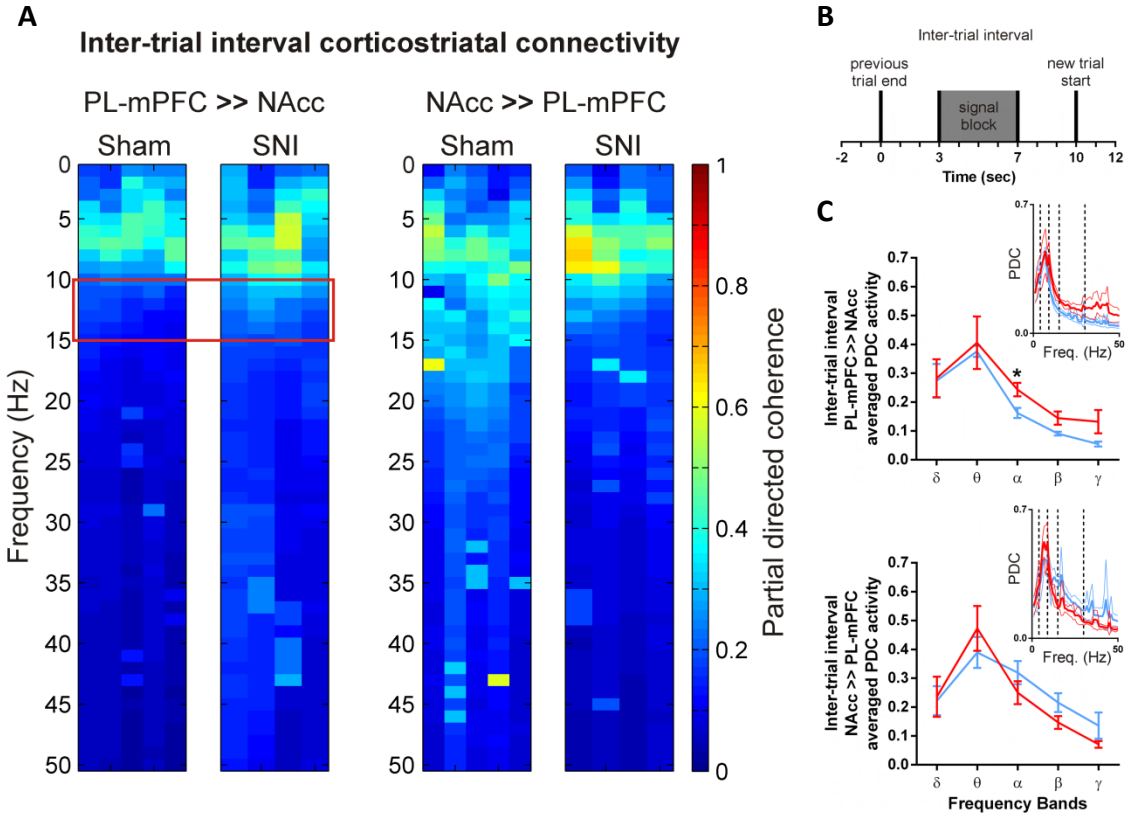

Figure 16 – SNI-treated animal showed a different corticostriatal connectivity profile when compared to controls. A, Bidirectional PDC activity during the ITI in Sham- and SNI-treated animals (bin resolution of 1 Hz). The red rectangle highlights the α frequency band, in which PDC values in the PL-mPFC>>NAcc direction were significantly higher for the SNI group. **B,** For the ITI PDC activity analysis, signal was extracted from 4 seconds of the ITI (represented in the scheme as signal block), from 3- and 6-second DNMS challenges. **C,** PDC values in the PL-mPFC>>NAcc (up) and NAcc>>PL-mPFC (down) directions, per frequency band. In the upper right corners, corresponding traces of PDC activity are represented (bin resolution of 1 Hz). Sham: n=5, SNI: n=4. Comparisons between groups and frequency bands were based on the two-way ANOVA (group x frequency band), followed by *post hoc* Bonferroni test. *p<0.05.

IV. Discussion

The present work contributed to the elucidation of how chronic pain impacts the normal functioning of the corticostriatal circuit and how these alterations affect the performance of a sWM task. The obtained results showed that (1) optogenetically inhibiting the corticostriatal circuit during the delay period of non-trained WM challenges resulted in a strong enhancement of the performance levels of SNI-treated animals, while not affecting the levels of Sham animals; (2) the selective inhibition of the circuit did not reveal antinociceptive effects; (3) the descending corticostriatal functional connectivity was constitutively altered in SNI-treated animals; (4) local firing activity in the PL-mPFC and NAcc was highly modulated by the execution of the sWM task in pre-trained paradigms; and (5) the corticostriatal functional connectivity in the θ frequency range was important for the correct execution of a pre-trained sWM task.

4.1. Optogenetic modulation of the corticostriatal circuit during the delay period of pre-trained DNMS challenges

Different studies in rodents showed that chronic pain associated with different etiologies resulted in impaired performance in tasks involving WM (Cain et al., 1997, Lindner et al., 1999, Leite-Almeida et al., 2009, Hu et al., 2010, Cardoso-Cruz et al., 2013a, Cardoso-Cruz et al., 2014). In the present study, it was observed that the performance levels of SNI-treated animals on pre-trained low-complexity DNMS challenges was not significantly impaired, suggesting that training might have resulted in the recovery of chronic pain-related WM deficits. In this regard, previous results evaluated DNMS task performance after the induction of the rat adjuvant arthritis model of chronic pain and showed that performance levels of chronic pain rats increased with training on the task (Cain et al., 1997, Lindner et al., 1999). WM deficits induced by the SNI model of neuropathic pain were also reduced in severity after several days of training in the T-maze and in the figure-8 maze sWM tasks (Cardoso-Cruz et al., 2013a, Cardoso-Cruz et al., 2014).

Repeated performance of a cognitive task results in a transition from flexible and attentive strategies to more automatic strategies to solve the task, possibly engaging different mechanisms (Gardner et al., 2013). Recent results showed that optogenetically suppressing mPFC activity during the delay period of a WM task did not have an impact in the performance

of well-trained animals (Liu et al., 2014). Similarly, the present study shows that optogenetic inhibition of the corticostriatal circuit did not have an impact in the performance levels of pre-trained low-complexity DNMS challenges. In addition and as expected, it did not significantly alter the number of omissions and the mean latency of choice response.

Chang and colleagues described correlated firing activity between mPFC and NAc neurons during cocaine-self administration, showing the importance of the communication between these two areas in reward-seeking behavior (Chang et al., 2000). Neuronal activity in these areas was also recorded during a WM task performance, in which rats had to press the matching lever. In both the mPFC and NAc regions, the authors identified neurons with delay period-related activity, with either increasing or decreasing firing patterns, during the whole delay period or during a specific portion of it (Chang et al., 2002). Interestingly, recordings from rat mPFC neuronal ensembles revealed that neuronal activity dynamically changed during the learning process of a figure-8 maze sWM task (Baeg et al., 2003).

The present results showed that the population firing activity of PL-mPFC and NAcc neurons was variable during the delay period of the DNMS task, according to what was previously described (Chang et al., 2002, Baeg et al., 2003). This pattern reflects the overall activity of the recorded neurons, which have distinct individual firing patterns. A slight increase in the population firing activity was evident in the SNI-treated animals in comparison with control animals. In addition, the results showed that partial optogenetic modulation of the corticostriatal circuit did not disrupt but induced slight changes in delay period firing dynamics. In this regard, it should be further noted that a strong reduction in population firing activity with optogenetic stimulation was not expected.

There is agreement in relation to the central role of the mPFC in decision-making (Miller and Cohen, 2001). The firing activity of mPFC neurons was shown to be modulated by the decision moment in different WM tasks (Baeg et al., 2003, Horst and Laubach, 2012, Cardoso-Cruz et al., 2013a). Specifically, it was shown that more mPFC neurons increase their firing rate in correct trials of a WM spatial navigation task, implicating this elevation of activity in successful decision making (Cardoso-Cruz et al., 2013a). Here, it was shown that the PL-mPFC population firing activity drastically increased in the choice moment of the DNMS task and that this pattern was not disrupted by the SNI lesion. The conservation of this pattern in animals with the SNI lesion has been previously reported in our laboratory in the execution of a figure-8 maze task (Cardoso-Cruz et al., 2013a).

The NAc is broadly involved in guiding behavior (Floresco, 2015) and its activity was long shown to be highly modulated by rewarding events and reward predictive cues, evolving during learning of a reward acquisition task (Miyazaki et al., 1998). The NAc is thought to be in

the interface between the limbic and motor systems, linking motivations with actions (Mogenson et al., 1993). Its activity was previously shown to be modulated by correct and incorrect responses in a WM task. Namely, its activity was increased before correct choices but not before incorrect choices (Chang et al., 2002). Similarly, a strong segregation of NAcc population firing activity during correct and incorrect trials was verified in the present work, with NAcc population firing activity showing an increase prior to a correct response and a decrease prior to an incorrect response. Importantly, segregation of NAcc activity in terms of correct and incorrect trials was not disrupted by the SNI lesion.

Theta oscillatory activity has a relevant role in learning and mnemonic processes (Buzsaki, 2002). Particularly, the entrainment of mPFC spiking activity to hippocampal θ-rhythm was shown to be important during WM decision-making (Jones and Wilson, 2005, Benchenane et al., 2010, Hyman et al., 2010). It has been reported that this synchronization was enhanced during correct WM decision-making and increased with learning (Benchenane et al., 2010, Hyman et al., 2010). In the NAc, oscillatory activity was shown to have a peak in the θ frequency band, during the performance of a radial arm maze task (Berke et al., 2004). Coherence between NAc spiking activity and the hippocampal θ rhythm was also increased during decision making (Berke et al., 2004, DeCoteau et al., 2007). Overall, these results show that, in both areas, demanding behavioral moments are transiently associated with increased coherence with a common ongoing hippocampal θ activity, which is thought to facilitate information transfer between coherent brain regions (Buzsaki, 2002). In the present study it is shown that the delay period of low-complexity pre-trained DNMS challenges was characterized by prominent power activity in the θ frequency range, in both the PL-mPFC and NAcc areas, which is in agreement with previous observations (Berke et al., 2004, Jones and Wilson, 2005, Benchenane et al., 2010, Hyman et al., 2010, Cardoso-Cruz et al., 2013a). The analysis of delay period corticostriatal COH2 revealed that phase-coupling between PL-mPFC and NAcc regions was stronger in the θ frequency band, which suggests potential coordinated information processing along the corticostriatal circuit in this frequency range. However, the COH2 analysis only indicates the extent of activity synchrony between the two areas, and does not inform of causal interactions between the two structures. This interaction was examined using the *partial directed coherence* (PDC) analysis, which is based on the principle of Granger causality and provides information about how the two structures are functionally connected (Sameshima and Baccalá, 1999). PDC analysis confirmed that corticostriatal connectivity was particularly high in the θ frequency range, across all tested conditions.

Several results support a role of functional connectivity in the mPFC networks during WM processes. It has been shown that before rats performed correct responses in a Y-maze WM

task, mPFC functional connectivity increased, but not before incorrect responses (Xie et al., 2014, Wei et al., 2015). The level of connectivity among local PFC neurons was altered during learning of a figure-8 maze task (Baeg et al., 2007). In this regard, WM deficits induced both by propofol anesthesia (Xu et al., 2013) or Alzheimer's disease (Liu et al., 2016) were shown to be associated with decreased PFC functional connectivity in the γ frequency band. Studies from our laboratory showed that chronic pain can lead to abnormally reduced functional connectivity, between the mPFC and the mediodorsal thalamus (Cardoso-Cruz et al., 2013b), and between the mPFC and hippocampus (Cardoso-Cruz et al., 2013a).

The present study showed that corticostriatal connectivity level in the θ frequency range was modulated by performance levels in low-complexity pre-trained DNMS paradigms, with a higher connectivity associated with a better performance. This strongly supports the importance of corticostriatal communication during WM performance. In addition, it is important to refer that corticostriatal functional connectivity in the ascending direction (from NAcc to PL-mPFC) was significantly higher in SNI animals when compared with control animals in the 6-second DNMS challenge without optical stimulation.

Overall, the optogenetic modulation of the corticostriatal circuit had no significant effects in the performance levels of low-complexity pre-trained DNMS challenges, which was associated with no significant effects in the firing and oscillatory patterns of the corticostriatal circuit. In spite of the lack of differences between SNI-treated animals and control animals in the performance of the task, important differences were found in the local corticostriatal firing activity patterns and corticostriatal connectivity during the DNMS task delay period.

4.2. Optogenetic modulation of the corticostriatal circuit during the delay period of non-trained DNMS challenges with increased complexity

The PFC is known to be particularly important in new and attention-demanding situations, mediating the ability to adapt to changing conditions (Miller and Cohen, 2001). PFC projections to the NAc, and particularly to the *core* region, were implicated in behavioral flexibility, integrating behavioral consequences to produce adequate behavior (Block et al., 2007). Lesion studies showed that the mPFC is important in the formation of associations between actions and consecutive outcomes, which underlies instrumental conditioning, but not in the maintenance and manifestation of such associations (Ostlund and Balleine, 2005). In respect to WM, while optogenetically suppressing mPFC activity during the delay period was shown to have no impact in the performance of pre-trained animals, it significantly impaired learning

and acquisition of a WM task (Liu et al., 2014). The corticostriatal circuitry is known to be broadly involved in mediating reward-seeking and goal-directed behavior (Miyazaki et al., 2004), which is essential to the execution of the DNMS task. In the present work it was shown that the optogenetic inhibition of the corticostriatal circuit during the execution of high-complexity non-trained DNMS challenges resulted in highly enhanced performance levels of the SNI-treated animals, but not of control animals. This suggests that corticostriatal adequate communication might be particularly relevant in WM, when more flexible and adaptive responses are required. In these challenges, performance levels decreased with increasing length of the delay period, nearing chance level. Optogenetic stimulation of the circuit prevented this decrease in SNI-treated animals. In spite of this effect on performance, the number of omissions and mean latency of choice response were not significantly altered. Notably, the mean latency levels were higher in high-complexity non-trained DNMS challenges when compared to pre-trained challenges, suggesting that overtraining resulted in optimized timing of responses.

4.3. The impact of optogenetic modulation of the corticostriatal circuit on nociception

Chronic pain induces general reorganization in the brain. The SNI model of neuropathic pain was shown to induce morphological and functional changes in the mPFC (Metz et al., 2009), and it leads to a decrease in prefrontal volume (Seminowicz et al., 2009). At the network level, resting state fMRI analysis showed that prolonged pain caused by the SNI lesion significantly altered connectivity patterns in the rat limbic system (Baliki et al., 2014). A broadband power increase was found both in neuropathic and inflammatory chronic pain models in the PFC and S1 brain regions (LeBlanc et al., 2016). Noteworthy, Baliki and colleagues found that increased corticostriatal functional connectivity in humans (mPFC and NAc) accurately predicted pain chronification (Baliki et al., 2012).

In the present study, SNI-treated animals were characterized by increased descending (from PL-mPFC to NAcc) corticostriatal functional connectivity in the α frequency range. Despite inherent differences between functional connectivity analysis in this study and in Baliki's study (Baliki et al., 2012), as well as the differences between rat and human homolog brain regions, the present results certainly support the possibility that similar mechanisms are occurring in the corticostriatal circuitry of both species in chronic pain conditions. It was recently proposed that abnormal integration of nociceptive inputs and contextual information during chronic

pain might be the consequence of altered information flow, in which disrupted oscillatory activity certainly has a contribution (Ploner et al., 2017). A mechanism for information flow in the brain was proposed, implicating α and β oscillations in the coding of predictions and γ oscillations in the coding of prediction errors (discrepancy between reality and predictions) (Bauer et al., 2014). Moreover, recent experimental evidence showed that top-down influences associated with prediction coding were mediated by increased functional connectivity in the α and β bands from higher to lower hierarchical brain areas, while bottom-up influences associated with prediction error coding were mediated by increased functional connectivity in the γ band from lower to higher brain areas (Michalareas et al., 2016). In this regard, the observed increased descending corticostriatal connectivity in the α frequency range might reflect a generalized abnormal descending information flow, associated with chronic pain (Ploner et al., 2017).

There is broad evidence for an altered activation state in different brain areas after the onset of chronic pain (Apkarian et al., 2005). In rats, both layers II/III of the ACC and PL-mPFC and layer V of the PL-mPFC were shown to have increased intrinsic excitability in chronic pain conditions. Optogenetically activating the infralimbic region of the mPFC had a facilitatory effect on pain (Ji and Neugebauer, 2012). Reversely, optogenetically inhibiting the ACC area of the mPFC resulted in strongly reduced pain perception (Gu et al., 2015). Layers II, V and VI of the mPFC strongly project to the NAcc, suggesting that PL-mPFC glutamatergic input to the NAcc might be altered in chronic pain conditions (Ding et al., 2001). Optogenetic activation of this circuit was shown to have anti-hyperalgesic effects in rats with neuropathic pain (Lee et al., 2015). Here, it was shown that the partial optogenetic inhibition of the corticostriatal circuit did not have a significant impact on the mechanical sensitivity threshold of both SNI and control animals. However, it should be noted that a tendency for an analgesic effect of the optogenetic inhibition was noted in both groups. In this regard, it should be considered that a higher intensity of light stimulation than the one used in the present protocol (5 mW) might have produced different results in behavioral performance and nociceptive responses.

V. Conclusions

In this study it was shown that the corticostriatal circuit had altered functionality during chronic pain. This conclusion is mainly supported by the observed differences in corticostriatal connectivity induced by chronic pain, and by a selective effect of the optogenetic modulation of the circuit on the WM performance level of SNI-treated animals. In specific, the following conclusions can be taken:

- The cognitive enhancement caused by the optogenetic modulation of the circuit was not mediated by a transient relief in pain levels. Instead, it is hypothesized that prolonged pain induces changes in corticostriatal activity, which are susceptible to modulation through optogenetic inhibition of the circuit. The most relevant evidence for this was the observation that the SNI lesion induced an increase in descending corticostriatal connectivity in the α frequency range.
- The cognitive enhancement caused by the optogenetic modulation of the circuit was restricted to high-complexity non-trained challenges. This suggests that, independently of equal underlying chronic pain-induced corticostriatal changes, the different novelty and complexity of the WM challenge differently engages the circuit.
- The analysis of the corticostriatal firing and oscillatory patterns during the performance of low-complexity pre-trained WM challenges highlighted the role of both the PL-mPFC and NAcc regions in critical epochs of the task, and revealed the importance of the corticostriatal functional connectivity in the θ frequency band for the correct performance of the WM task. These findings might be common to high-complexity non-trained challenges. However, learning might have a modulatory effect in the corticostriatal neuronal activity.
- The neuronal activity of SNI-treated animals was slightly increased during the delay period of low-complexity pre-trained DNMS challenges, and descending corticostriatal functional connectivity in the θ frequency band was found to be increased in SNI-treated animals. These changes are probably common to high-complexity non-trained challenges, which supports the idea that the observed enhancement in performance levels is related to chronic pain-induced changes in corticostriatal activity.

Investigation of the neuronal correlates of the corticostriatal activity during high-complexity non-trained DNMS challenges would provide a better insight into the exact mechanisms by which performance is enhanced by optogenetic modulation. In addition, optogenetically activating the corticostriatal circuit during the performance of the same DNMS challenges would certainly further contribute to the elucidation of how neuropathic pain influences the role of the corticostriatal circuit during WM information processing.

VI. Bibliography

Aguiar P, Mendonça L, Galhardo V (2007) OpenControl: A free opensource software for video tracking and automated control of behavioral mazes. Journal of Neuroscience Methods 166:66-72.

Apkarian AV, Baliki MN, Farmer MA (2012) Predicting transition to chronic pain. Current opinion in neurology 26:360-367.

Apkarian AV, Baliki MN, Geha PY (2009) Towards a theory of chronic pain. Prog Neurobiol 87:81-97.

Apkarian AV, Bushnell MC, Treede RD, Zubieta JK (2005) Human brain mechanisms of pain perception and regulation in health and disease. European journal of pain (London, England) 9:463-484.

Apkarian AV, Sosa Y, Sonty S, Levy RM, Harden RN, Parrish TB, Gitelman DR (2004) Chronic back pain is associated with decreased prefrontal and thalamic gray matter density. J Neurosci 24:10410-10415.

Apkarian AV, Thomas PS, Krauss BR, Szeverenyi NM (2001) Prefrontal cortical hyperactivity in patients with sympathetically mediated chronic pain. Neuroscience letters 311:193-197.

Baddeley A (2012) Working memory: theories, models, and controversies. Annu Rev Psychol 63:1-29.

Baeg EH, Kim YB, Huh K, Mook-Jung I, Kim HT, Jung MW (2003) Dynamics of Population Code for Working Memory in the Prefrontal Cortex. Neuron 40:177-188.

Baeg EH, Kim YB, Kim J, Ghim JW, Kim JJ, Jung MW (2007) Learning-induced enduring changes in functional connectivity among prefrontal cortical neurons. J Neurosci 27:909-918.

Baliki MN, Chang PC, Baria AT, Centeno MV, Apkarian AV (2014) Resting-sate functional reorganization of the rat limbic system following neuropathic injury. Scientific Reports 4:6186.

Baliki MN, Chialvo DR, Geha PY, Levy RM, Harden RN, Parrish TB, Apkarian AV (2006) Chronic pain and the emotional brain: specific brain activity associated with spontaneous fluctuations of intensity of chronic back pain. J Neurosci 26:12165-12173.

Baliki MN, Geha PY, Fields HL, Apkarian AV (2010) Predicting value of pain and analgesia: nucleus accumbens response to noxious stimuli changes in the presence of chronic pain. Neuron 66:149-160.

Baliki MN, Mansour A, Baria AT, Huang L, Berger SE, Fields HL, Apkarian AV (2013) Parceling human accumbens into putative core and shell dissociates encoding of values for reward and pain. J Neurosci 33:16383-16393.

Baliki MN, Petre B, Torbey S, Herrmann KM, Huang L, Schnitzer TJ, Fields HL, Apkarian AV (2012) Corticostriatal functional connectivity predicts transition to chronic back pain. Nat Neurosci 15:1117-1119.

Bauer M, Stenner MP, Friston KJ, Dolan RJ (2014) Attentional modulation of alpha/beta and gamma oscillations reflect functionally distinct processes. J Neurosci 34:16117-16125.

Bauer RH, Fuster JM (1976) Delayed-matching and delayed-response deficit from cooling dorsolateral prefrontal cortex in monkeys. Journal of comparative and physiological psychology 90:293-302.

Becerra L, Borsook D (2008) Signal valence in the nucleus accumbens to pain onset and offset. European journal of pain (London, England) 12:866-869.

Becerra L, Navratilova E, Porreca F, Borsook D (2013) Analogous responses in the nucleus accumbens and cingulate cortex to pain onset (aversion) and offset (relief) in rats and humans. J Neurophysiol 110:1221-1226.

Benchenane K, Peyrache A, Khamassi M, Tierney PL, Gioanni Y, Battaglia FP, Wiener SI (2010) Coherent theta oscillations and reorganization of spike timing in the hippocampal-prefrontal network upon learning. Neuron 66:921-936.

Bennett GJ, Xie YK (1988) A peripheral mononeuropathy in rat that produces disorders of pain sensation like those seen in man. Pain 33:87-107.

Berke JD, Okatan M, Skurski J, Eichenbaum HB (2004) Oscillatory entrainment of striatal neurons in freely moving rats. Neuron 43:883-896.

Block AE, Dhanji H, Thompson-Tardif SF, Floresco SB (2007) Thalamic-prefrontal cortical-ventral striatal circuitry mediates dissociable components of strategy set shifting. Cerebral cortex (New York, NY : 1991) 17:1625-1636.

Blom SM, Pfister J-P, Santello M, Senn W, Nevian T (2014) Nerve Injury-Induced Neuropathic Pain Causes Disinhibition of the Anterior Cingulate Cortex. The Journal of Neuroscience 34:5754-5764.

Boyden ES, Zhang F, Bamberg E, Nagel G, Deisseroth K (2005) Millisecond-timescale, genetically targeted optical control of neural activity. Nat Neurosci 8:1263-1268.

Britt JP, Benaliouad F, McDevitt RA, Stuber GD, Wise RA, Bonci A (2012) Synaptic and behavioral profile of multiple glutamatergic inputs to the nucleus accumbens. Neuron 76:790-803.

Burstein R, Giesler GJ (1989) Retrograde labeling of neurons in spinal cord that project directly to nucleus accumbens or the septal nuclei in the rat. Brain Research 497:149-154.

Bushnell MC, Ceko M, Low LA (2013) Cognitive and emotional control of pain and its disruption in chronic pain. Nat Rev Neurosci 14:502-511.

Buzsaki G (2002) Theta oscillations in the hippocampus. Neuron 33:325-340.

Cain CK, Francis JM, Plone MA, Emerich DF, Lindner MD (1997) Pain-related disability and effects of chronic morphine in the adjuvant-induced arthritis model of chronic pain. Physiol Behav 62:199-205.

Cardoso-Cruz H, Dourado M, Monteiro C, Matos MR, Galhardo V (2014) Activation of dopaminergic D2/D3 receptors modulates dorsoventral connectivity in the hippocampus and reverses the impairment of working memory after nerve injury. J Neurosci 34:5861-5873.

Cardoso-Cruz H, Lima D, Galhardo V (2011) Instability of spatial encoding by CA1 hippocampal place cells after peripheral nerve injury. Eur J Neurosci 33:2255-2264.

Cardoso-Cruz H, Lima D, Galhardo V (2013a) Impaired spatial memory performance in a rat model of neuropathic pain is associated with reduced hippocampus-prefrontal cortex connectivity. J Neurosci 33:2465-2480.

Cardoso-Cruz H, Sousa M, Vieira JB, Lima D, Galhardo V (2013b) Prefrontal cortex and mediodorsal thalamus reduced connectivity is associated with spatial working memory impairment in rats with inflammatory pain. Pain 154:2397-2406.

Carter ME, de Lecea L (2011) Optogenetic investigation of neural circuits in vivo. Trends in molecular medicine 17:197-206.

Chang JY, Chen L, Luo F, Shi LH, Woodward DJ (2002) Neuronal responses in the frontal cortico-basal ganglia system during delayed matching-to-sample task: ensemble recording in freely moving rats. Experimental brain research 142:67-80.

Chang JY, Janak PH, Woodward DJ (2000) Neuronal and behavioral correlations in the medial prefrontal cortex and nucleus accumbens during cocaine self-administration by rats. Neuroscience 99:433-443.

Chang PC, Pollema-Mays SL, Centeno MV, Procissi D, Contini M, Baria AT, Martina M, Apkarian AV (2014) Role of nucleus accumbens in neuropathic pain: linked multi-scale evidence in the rat transitioning to neuropathic pain. Pain 155:1128-1139.

Chaplan SR, Bach FW, Pogrel JW, Chung JM, Yaksh TL (1994) Quantitative assessment of tactile allodynia in the rat paw. J Neurosci Methods 53:55-63.

Christophel TB, Klink PC, Spitzer B, Roelfsema PR, Haynes JD (2017) The Distributed Nature of Working Memory. Trends Cogn Sci 21:111-124.

Clements IP, Gnade AG, Rush AD, Patten CD, Twomey MC, Kravitz AV (2013) Miniaturized LED sources for in vivo optogenetic experimentation. vol. 8586, pp 85860X-85860X-85869.

Cordeiro Matos S, Zhang Z (2015) Peripheral Neuropathy Induces HCN Channel Dysfunction in Pyramidal Neurons of the Medial Prefrontal Cortex. 35:13244-13256.

Costigan M, Scholz J, Woolf CJ (2009) Neuropathic pain: a maladaptive response of the nervous system to damage. Annu Rev Neurosci 32:1-32.

Courtney SM, Ungerleider LG, Keil K, Haxby JV (1997) Transient and sustained activity in a distributed neural system for human working memory. Nature 386:608-611.

D'Esposito M, Postle BR (2015) The cognitive neuroscience of working memory. Annu Rev Psychol 66:115-142.

Decosterd I, Woolf CJ (2000) Spared nerve injury: an animal model of persistent peripheral neuropathic pain. Pain 87:149-158.

DeCoteau WE, Thorn C, Gibson DJ, Courtemanche R, Mitra P, Kubota Y, Graybiel AM (2007) Learning-related coordination of striatal and hippocampal theta rhythms during acquisition of a procedural maze task. Proc Natl Acad Sci U S A 104:5644-5649.

Delatour B, Gisquet-Verrier P (1996) Prelimbic cortex specific lesions disrupt delayed-variable response tasks in the rat. Behav Neurosci 110:1282-1298.

Dick BD, Rashiq S (2007) Disruption of attention and working memory traces in individuals with chronic pain. Anesthesia and analgesia 104:1223-1229, tables of contents.

Diester I, Kaufman MT, Mogri M, Pashaie R, Goo W, Yizhar O, Ramakrishnan C, Deisseroth K, Shenoy KV (2011) An optogenetic toolbox designed for primates. Nat Neurosci 14:387-397.

Ding DC, Gabbott PL, Totterdell S (2001) Differences in the laminar origin of projections from the medial prefrontal cortex to the nucleus accumbens shell and core regions in the rat. Brain Res 917:81-89.

Dixon WJ (1980) Efficient analysis of experimental observations. Annual review of pharmacology and toxicology 20:441-462.

Dunnett SB, Nathwani F, Brasted PJ (1999) Medial prefrontal and neostriatal lesions disrupt performance in an operant delayed alternation task in rats. Behavioural brain research 106:13-28.

Eccleston C, Crombez G (1999) Pain demands attention: a cognitive-affective model of the interruptive function of pain. Psychological bulletin 125:356-366.

Fenno L, Yizhar O, Deisseroth K (2011) The development and application of optogenetics. Annu Rev Neurosci 34:389-412.

Floresco SB (2015) The nucleus accumbens: an interface between cognition, emotion, and action. Annu Rev Psychol 66:25-52.

Floresco SB, Braaksma DN, Phillips AG (1999) Thalamic-cortical-striatal circuitry subserves working memory during delayed responding on a radial arm maze. J Neurosci 19:11061-11071.

Fries P (2005) A mechanism for cognitive dynamics: neuronal communication through neuronal coherence. Trends Cogn Sci 9:474-480.

Fritts ME, Asbury ET, Horton JE, Isaac WL (1998) Medial prefrontal lesion deficits involving or sparing the prelimbic area in the rat. Physiol Behav 64:373-380.

Fuchs PN, Peng YB, Boyette-Davis JA, Uhelski ML (2014) The anterior cingulate cortex and pain processing. Frontiers in Integrative Neuroscience 8:35.

Funahashi S, Bruce CJ, Goldman-Rakic PS (1989) Mnemonic coding of visual space in the monkey's dorsolateral prefrontal cortex. J Neurophysiol 61:331-349.

Funahashi S, Bruce CJ, Goldman-Rakic PS (1993) Dorsolateral prefrontal lesions and oculomotor delayed-response performance: evidence for mnemonic "scotomas". J Neurosci 13:1479-1497.

Fuster JM, Alexander GE (1971) Neuron activity related to short-term memory. Science (New York, NY) 173:652-654.

Gal G, Joel D, Gusak O, Feldon J, Weiner I (1997) The effects of electrolytic lesion to the shell subterritory of the nucleus accumbens on delayed non-matching-to-sample and four-arm baited eight-arm radial-maze tasks. Behav Neurosci 111:92-103.

Gardner RS, Uttaro MR, Fleming SE, Suarez DF, Ascoli GA, Dumas TC (2013) A secondary working memory challenge preserves primary place strategies despite overtraining. Learning & memory (Cold Spring Harbor, NY) 20:648-656.

Gazzaley A, Nobre AC (2012) Top-down modulation: bridging selective attention and working memory. Trends Cogn Sci 16:129-135.

Gazzaley A, Rissman J, D'esposito M (2004) Functional connectivity during working memory maintenance. Cognitive, Affective, & Behavioral Neuroscience 4:580-599.

Goldman-Rakic PS (1987) Circuitry of Primate Prefrontal Cortex and Regulation of Behavior by Representational Memory. In: Comprehensive Physiology: John Wiley & Sons, Inc.

Gradinaru V, Zhang F, Ramakrishnan C, Mattis J, Prakash R, Diester I, Goshen I, Thompson KR, Deisseroth K (2010) Molecular and Cellular Approaches for Diversifying and Extending Optogenetics. Cell 141:154-165.

Granon S, Vidal C, Thinus-Blanc C, Changeux JP, Poucet B (1994) Working memory, response selection, and effortful processing in rats with medial prefrontal lesions. Behav Neurosci 108:883-891.

Gu L, Uhelski ML, Anand S, Romero-Ortega M, Kim Y-t, Fuchs PN, Mohanty SK (2015) Pain Inhibition by Optogenetic Activation of Specific Anterior Cingulate Cortical Neurons. PLoS ONE 10:e0117746.

Gunaydin LA, Yizhar O, Berndt A, Sohal VS, Deisseroth K, Hegemann P (2010) Ultrafast optogenetic control. Nat Neurosci 13:387-392.

Harrison SA, Tong F (2009) Decoding reveals the contents of visual working memory in early visual areas. Nature 458:632-635.

Hart RP, Martelli MF, Zasler ND (2000) Chronic pain and neuropsychological functioning. Neuropsychology review 10:131-149.

Heidbreder CA, Groenewegen HJ (2003) The medial prefrontal cortex in the rat: evidence for a dorso-ventral distinction based upon functional and anatomical characteristics. Neurosci Biobehav Rev 27:555-579.

Horst NK, Laubach M (2012) Working with memory: evidence for a role for the medial prefrontal cortex in performance monitoring during spatial delayed alternation. J Neurophysiol 108:3276-3288.

Hu Y, Yang J, Hu Y, Wang Y, Li W (2010) Amitriptyline rather than lornoxicam ameliorates neuropathic pain-induced deficits in abilities of spatial learning and memory. Eur J Anaesthesiol 27:162-168.

Hyman JM, Zilli EA, Paley AM, Hasselmo ME (2005) Medial prefrontal cortex cells show dynamic modulation with the hippocampal theta rhythm dependent on behavior. Hippocampus 15:739-749.

Hyman JM, Zilli EA, Paley AM, Hasselmo ME (2010) Working Memory Performance Correlates with Prefrontal-Hippocampal Theta Interactions but not with Prefrontal Neuron Firing Rates. Front Integr Neurosci 4:2.

Jacobsen CF (1935) Functions of frontal association area in primates. Archives of Neurology & Psychiatry 33:558-569.

Jaggi AS, Jain V, Singh N (2011) Animal models of neuropathic pain. Fundamental & clinical pharmacology 25:1-28.

Jamison RN, Sbrocco T, Parris WC (1988) The influence of problems with concentration and memory on emotional distress and daily activities in chronic pain patients. International journal of psychiatry in medicine 18:183-191.

Jensen TS, Baron R, Haanpaa M, Kalso E, Loeser JD, Rice AS, Treede RD (2011) A new definition of neuropathic pain. Pain 152:2204-2205.

Ji G, Neugebauer V (2012) Modulation of medial prefrontal cortical activity using in vivo recordings and optogenetics. Mol Brain 5:36.

Jones MW, Wilson MA (2005) Theta rhythms coordinate hippocampal-prefrontal interactions in a spatial memory task. PLoS biology 3:e402.

Jongen-Relo AL, Kaufmann S, Feldon J (2003) A differential involvement of the shell and core subterritories of the nucleus accumbens of rats in memory processes. Behav Neurosci 117:150-168.

Kim SH, Chung JM (1992) An experimental model for peripheral neuropathy produced by segmental spinal nerve ligation in the rat. Pain 50:355-363.

Kimberg DY, D'Esposito (1997) Cognitive functions in the prefrontal cortex: working memory and executive control. Current Directions in Psychological Science.

Kolb B, Buhrmann K, McDonald R, Sutherland RJ (1994) Dissociation of the medial prefrontal, posterior parietal, and posterior temporal cortex for spatial navigation and recognition memory in the rat. Cerebral cortex (New York, NY : 1991) 4:664-680.

Kuner R, Flor H (2017) Structural plasticity and reorganisation in chronic pain. Nat Rev Neurosci 18:20-30.

LeBlanc BW, Bowary PM, Chao YC, Lii TR, Saab CY (2016) Electroencephalographic signatures of pain and analgesia in rats. Pain 157:2330-2340.

Lee DM, Pendleton N, Tajar A, O'Neill TW, O'Connor DB, Bartfai G, Boonen S, Casanueva FF, Finn JD, Forti G, Giwercman A, Han TS, Huhtaniemi IT, Kula K, Lean ME, Punab M, Silman AJ, Vanderschueren D, Moseley CM, Wu FC, McBeth J (2010) Chronic widespread pain is associated with slower cognitive processing speed in middle-aged and older European men. Pain 151:30-36.

Lee M, Manders TR, Eberle SE, Su C, D'Amour J, Yang R, Lin HY, Deisseroth K, Froemke RC, Wang J (2015) Activation of corticostriatal circuitry relieves chronic neuropathic pain. J Neurosci 35:5247-5259.

Leite-Almeida H, Almeida-Torres L, Mesquita AR, Pertovaara A, Sousa N, Cerqueira JJ, Almeida A (2009) The impact of age on emotional and cognitive behaviours triggered by experimental neuropathy in rats. Pain 144:57-65.

Lewis SJ, Dove A, Robbins TW, Barker RA, Owen AM (2004) Striatal contributions to working memory: a functional magnetic resonance imaging study in humans. Eur J Neurosci 19:755-760.

Lindner MD, Plone MA, Francis JM, Cain CK (1999) Chronic morphine reduces pain-related disability in a rodent model of chronic, inflammatory pain. Exp Clin Psychopharmacol 7:187-197.

Liu D, Gu X, Zhu J, Zhang X, Han Z, Yan W, Cheng Q, Hao J, Fan H, Hou R, Chen Z, Chen Y, Li CT (2014) Medial prefrontal activity during delay period contributes to learning of a working memory task. Science (New York, NY) 346:458-463.

Liu T, Bai W, Wang J, Tian X (2016) An aberrant link between gamma oscillation and functional connectivity in Abeta1-42-mediated memory deficits in rats. Behavioural brain research 297:51-58.

Lorenz J, Cross DJ, Minoshima S, Morrow TJ, Paulson PE, Casey KL (2002) A unique representation of heat allodynia in the human brain. Neuron 35:383-393.

Luo C, Kuner T, Kuner R (2014) Synaptic plasticity in pathological pain. Trends in neurosciences 37:343-355.

Luo L, Callaway EM, Svoboda K (2008) Genetic Dissection of Neural Circuits. Neuron 57:634-660.

Matsuno-Yagi A, Mukohata Y (1977) Two possible roles of bacteriorhodopsin; a comparative study of strains of Halobacterium halobium differing in pigmentation. Biochemical and biophysical research communications 78:237-243.

Melzack R, Wall PD (1965) Pain mechanisms: a new theory. Science (New York, NY) 150:971-979.

Metz AE, Yau HJ, Centeno MV, Apkarian AV, Martina M (2009) Morphological and functional reorganization of rat medial prefrontal cortex in neuropathic pain. Proc Natl Acad Sci U S A 106:2423-2428.

Michalareas G, Vezoli J, van Pelt S, Schoffelen JM, Kennedy H, Fries P (2016) Alpha-Beta and Gamma Rhythms Subserve Feedback and Feedforward Influences among Human Visual Cortical Areas. Neuron 89:384-397.

Millecamps M, Centeno MV, Berra HH, Rudick CN, Lavarello S, Tkatch T, Apkarian AV (2007) D-cycloserine reduces neuropathic pain behavior through limbic NMDA-mediated circuitry. Pain 132:108-123.

Miller EK, Cohen JD (2001) An integrative theory of prefrontal cortex function. Annu Rev Neurosci 24:167-202.

Miller EK, Erickson CA, Desimone R (1996) Neural mechanisms of visual working memory in prefrontal cortex of the macaque. J Neurosci 16:5154-5167.

Miyazaki K, Mogi E, Araki N, Matsumoto G (1998) Reward-quality dependent anticipation in rat nucleus accumbens. Neuroreport 9:3943-3948.

Miyazaki K, W Miyazaki K, Matsumoto G (2004) Different representation of forthcoming reward in nucleus accumbens and medial prefrontal cortex.

Mogenson GJ, Brudzynski S, Wu M (1993) From motivation to action: a review of dopaminergic regulation of limbic→nucleus accumbens→ventral pallidum→pedunculopontine nucleus circuitries involved in limbic-motor integration.

Mohanty SK, Lakshminarayananan V (2015) Optical Techniques in Optogenetics. Journal of modern optics 62:949-970.

Moriarty O, McGuire BE, Finn DP (2011) The effect of pain on cognitive function: a review of clinical and preclinical research. Prog Neurobiol 93:385-404.

Morris RG, Hagan JJ, Rawlins JN (1986) Allocentric spatial learning by hippocampectomised rats: a further test of the "spatial mapping" and "working memory" theories of hippocampal function. The Quarterly journal of experimental psychology B, Comparative and physiological psychology 38:365-395.

Mosconi T, Kruger L (1996) Fixed-diameter polyethylene cuffs applied to the rat sciatic nerve induce a painful neuropathy: ultrastructural morphometric analysis of axonal alterations. Pain 64:37-57.

Muller NG, Machado L, Knight RT (2002) Contributions of subregions of the prefrontal cortex to working memory: evidence from brain lesions in humans. Journal of cognitive neuroscience 14:673-686.

Nagel G, Ollig D, Fuhrmann M, Kateriya S, Musti AM, Bamberg E, Hegemann P (2002) Channelrhodopsin-1: a light-gated proton channel in green algae. Science (New York, NY) 296:2395-2398.

Navratilova E, Xie JY, Okun A, Qu C, Eyde N, Ci S, Ossipov MH, King T, Fields HL, Porreca F (2012) Pain relief produces negative reinforcement through activation of mesolimbic reward-valuation circuitry. Proc Natl Acad Sci U S A 109:20709-20713.

Neugebauer V, Galhardo V, Maione S, Mackey SC (2009) Forebrain Pain Mechanisms. Brain research reviews 60:226-242.

Newman HM, Stevens RT, Apkarian AV (1996) Direct spinal projections to limbic and striatal areas: anterograde transport studies from the upper cervical spinal cord and the cervical enlargement in squirrel monkey and rat. J Comp Neurol 365:640-658.

O'Neill P-K, Gordon JA, Sigurdsson T (2013) Theta Oscillations in the Medial Prefrontal Cortex Are Modulated by Spatial Working Memory and Synchronize with the Hippocampus through Its Ventral Subregion. The Journal of Neuroscience 33:14211-14224.

Oesterhelt D, Stoeckenius W (1971) Rhodopsin-like protein from the purple membrane of Halobacterium halobium. Nature: New biology 233:149-152.

Olton DS, Becker JT, Handelmann GE (1979) Hippocampus, space, and memory. Behavioral and Brain Sciences 2:313-322.

Oosterman JM, Derksen LC, van Wijck AJ, Veldhuijzen DS, Kessels RP (2011) Memory functions in chronic pain: examining contributions of attention and age to test performance. The Clinical journal of pain 27:70-75.

Oosterman JM, Dijkerman HC, Kessels RP, Scherder EJ (2010) A unique association between cognitive inhibition and pain sensitivity in healthy participants. European journal of pain (London, England) 14:1046-1050.

Ostlund SB, Balleine BW (2005) Lesions of medial prefrontal cortex disrupt the acquisition but not the expression of goal-directed learning. J Neurosci 25:7763-7770.

Palva JM, Monto S, Kulashekhar S, Palva S (2010) Neuronal synchrony reveals working memory networks and predicts individual memory capacity. Proc Natl Acad Sci U S A 107:7580-7585.

Pare D, Gaudreau H (1996) Projection cells and interneurons of the lateral and basolateral amygdala: distinct firing patterns and differential relation to theta and delta rhythms in conscious cats. J Neurosci 16:3334-3350.

Pierce KL, Premont RT, Lefkowitz RJ (2002) Seven-transmembrane receptors. Nature reviews Molecular cell biology 3:639-650.

Ploner M, Sorg C, Gross J (2017) Brain Rhythms of Pain. Trends in Cognitive Sciences 21:100-110.

Porro CA, Baraldi P, Pagnoni G, Serafini M, Facchin P, Maieron M, Nichelli P (2002) Does anticipation of pain affect cortical nociceptive systems? J Neurosci 22:3206-3214.

Porter MC, Mair RG (1997) The effects of frontal cortical lesions on remembering depend on the procedural demands of tasks performed in the radial arm maze. Behavioural brain research 87:115-125.

Price DD (2000) Psychological and neural mechanisms of the affective dimension of pain. Science (New York, NY) 288:1769-1772.

Ragozzino ME, Adams S, Kesner RP (1998) Differential involvement of the dorsal anterior cingulate and prelimbic-infralimbic areas of the rodent prefrontal cortex in spatial working memory. Behav Neurosci 112:293-303.

Ren W-J, Liu Y, Zhou L-J, Li W, Zhong Y, Pang R-P, Xin W-J, Wei X-H, Wang J, Zhu H-Q, Wu C-Y, Qin Z-H, Liu G, Liu X-G (2011) Peripheral Nerve Injury Leads to Working Memory Deficits and Dysfunction of the Hippocampus by Upregulation of TNF-α in Rodents. Neuropsychopharmacology : official publication of the American College of Neuropsychopharmacology 36:979-992.

Ren W, Centeno MV, Berger S, Wu Y, Na X, Liu X, Kondapalli J, Apkarian AV, Martina M, Surmeier DJ (2016) The indirect pathway of the nucleus accumbens shell amplifies neuropathic pain. Nat Neurosci 19:220-222.

Riley MR, Constantinidis C (2015) Role of Prefrontal Persistent Activity in Working Memory. Frontiers in systems neuroscience 9:181.

Roux F, Uhlhaas PJ (2014) Working memory and neural oscillations: alpha-gamma versus theta-gamma codes for distinct WM information? Trends Cogn Sci 18:16-25.

S. Olton D, J. Samuelson R (1976) Remembrance of places passed: Spatial memory in rats.

Salazar RF, Dotson NM, Bressler SL, Gray CM (2012) Content-specific fronto-parietal synchronization during visual working memory. Science (New York, NY) 338:1097-1100.

Sameshima K, Baccalá LA (1999) Using partial directed coherence to describe neuronal ensemble interactions. Journal of Neuroscience Methods 94:93-103.

Sanchez-Santed F, de Bruin JP, Heinsbroek RP, Verwer RW (1997) Spatial delayed alternation of rats in a T-maze: effects of neurotoxic lesions of the medial prefrontal cortex and of T-maze rotations. Behavioural brain research 84:73-79.

Sarkis R, Saade N, Atweh S, Jabbur S, Al-Amin H (2011) Chronic dizocilpine or apomorphine and development of neuropathy in two rat models I: behavioral effects and role of nucleus accumbens. Exp Neurol 228:19-29.

Schultz W (2013) Updating dopamine reward signals. Current opinion in neurobiology 23:229-238.

Seamans JK, Floresco SB, Phillips AG (1995) Functional differences between the prelimbic and anterior cingulate regions of the rat prefrontal cortex. Behav Neurosci 109:1063-1073.

Seamans JK, Phillips AG (1994) Selective memory impairments produced by transient lidocaine-induced lesions of the nucleus accumbens in rats. Behav Neurosci 108:456-468.

Seltzer Z, Dubner R, Shir Y (1990) A novel behavioral model of neuropathic pain disorders produced in rats by partial sciatic nerve injury. Pain 43:205-218.

Seminowicz DA, Laferriere AL, Millecamps M, Yu JS, Coderre TJ, Bushnell MC (2009) MRI structural brain changes associated with sensory and emotional function in a rat model of long-term neuropathic pain. Neuroimage 47:1007-1014.

Siapas AG, Lubenov EV, Wilson MA (2005) Prefrontal phase locking to hippocampal theta oscillations. Neuron 46:141-151.

Tracey I, Mantyh PW The Cerebral Signature for Pain Perception and Its Modulation. Neuron 55:377-391.

Vadakkan KI, Jia YH, Zhuo M (2005) A behavioral model of neuropathic pain induced by ligation of the common peroneal nerve in mice. The journal of pain : official journal of the American Pain Society 6:747-756.

Vertes RP (2003) Differential projections of the infralimbic and prelimbic cortex in the rat. Synapse 51:32-58.

Villemure C, Laferriere AC, Bushnell MC (2012) The ventral striatum is implicated in the analgesic effect of mood changes. Pain research & management 17:69-74.

von Hehn CA, Baron R, Woolf CJ (2012) Deconstructing the neuropathic pain phenotype to reveal neural mechanisms. Neuron 73:638-652.

Voytek B, Knight RT (2010) Prefrontal cortex and basal ganglia contributions to visual working memory. Proceedings of the National Academy of Sciences of the United States of America 107:18167-18172.

Wager TD, Davidson ML, Hughes BL, Lindquist MA, Ochsner KN (2008) Prefrontal-subcortical pathways mediating successful emotion regulation. Neuron 59:1037-1050.

Wager TD, Rilling JK, Smith EE, Sokolik A, Casey KL, Davidson RJ, Kosslyn SM, Rose RM, Cohen JD (2004) Placebo-induced changes in FMRI in the anticipation and experience of pain. Science (New York, NY) 303:1162-1167.

Wall PD, Devor M, Inbal R, Scadding JW, Schonfeld D, Seltzer Z, Tomkiewicz MM (1979) Autotomy following peripheral nerve lesions: experimental anaesthesia dolorosa. Pain 7:103-111.

Wall PD, Gutnick M (1974) Properties of afferent nerve impulses originating from a neuroma. Nature 248:740-743.

Wang GQ, Cen C, Li C, Cao S, Wang N, Zhou Z, Liu XM, Xu Y, Tian NX, Zhang Y, Wang J, Wang LP, Wang Y (2015) Deactivation of excitatory neurons in the prelimbic cortex via Cdk5 promotes pain sensation and anxiety. Nat Commun 6:7660.

Wei J, Bai W, Liu T, Tian X (2015) Functional connectivity changes during a working memory task in rat via NMF analysis. Frontiers in behavioral neuroscience 9:2.

Weiner DK, Rudy TE, Morrow L, Slaboda J, Lieber S (2006) The relationship between pain, neuropsychological performance, and physical function in community-dwelling older adults with chronic low back pain. Pain medicine (Malden, Mass) 7:60-70.

Woolf CJ (2011) Central sensitization: implications for the diagnosis and treatment of pain. Pain 152:S2-15.

Wu XB, Liang B, Gao YJ (2016) The increase of intrinsic excitability of layer V pyramidal cells in the prelimbic medial prefrontal cortex of adult mice after peripheral inflammation. Neuroscience letters 611:40-45.

Xie J, Bai W, Liu T, Tian X (2014) Functional connectivity among spike trains in neural assemblies during rat working memory task. Behavioural brain research 274:248-257.

Xu X, Tian Y, Li S, Li Y, Wang G, Tian X (2013) Inhibition of propofol anesthesia on functional connectivity between LFPs in PFC during rat working memory task. PLoS One 8:e83653.

Yizhar O, Fenno Lief E, Davidson Thomas J, Mogri M, Deisseroth K (2011) Optogenetics in Neural Systems. Neuron 71:9-34.

Zahm DS, Brog JS (1992) On the significance of subterritories in the "accumbens" part of the rat ventral striatum. Neuroscience 50:751-767.

Zhang F, Gradinaru V, Adamantidis AR, Durand R, Airan RD, de Lecea L, Deisseroth K (2010) Optogenetic interrogation of neural circuits: technology for probing mammalian brain structures. Nat Protocols 5:439-456.

Zhang F, Vierock J, Yizhar O, Fenno LE, Tsunoda S, Kianianmomeni A, Prigge M, Berndt A, Cushman J, Polle J, Magnuson J, Hegemann P, Deisseroth K (2011) The Microbial Opsin Family of Optogenetic Tools. Cell 147:1446-1457.

Zhang Z, Gadotti VM, Chen L, Souza IA, Stemkowski PL, Zamponi GW (2015) Role of Prelimbic GABAergic Circuits in Sensory and Emotional Aspects of Neuropathic Pain. Cell Rep 12:752-759.

Zhuo M (2008) Cortical excitation and chronic pain. Trends in neurosciences 31:199-207.